



PII S0016-7037(97)00176-2

Experiments on the role of water in petroleum formation

M. D. LEWAN

U.S. Geological Survey, Box 25046, MS977, Denver Federal Center, Denver, Colorado 80225, USA

(Received April 23, 1996; accepted in revised form April 25, 1997)

Abstract—Pyrolysis experiments were conducted on immature petroleum source rocks under various conditions to evaluate the role of water in petroleum formation. At temperatures less than 330°C for 72 h, the thermal decomposition of kerogen to bitumen was not significantly affected by the presence or absence of liquid water in contact with heated gravel-sized source rock. However, at 330 and 350°C for 72 h, the thermal decomposition of generated bitumen was significantly affected by the presence or absence of liquid water. Carbon-carbon bond cross linking resulting in the formation of an insoluble bitumen (i.e., pyrobitumen) is the dominant reaction pathway in the absence of liquid water. Conversely, thermal cracking of carbon-carbon bonds resulting in the generation of saturate-enriched oil, which is similar to natural crude oils, is the dominant reaction pathway in the presence of liquid water. This difference in reaction pathways is explained by the availability of an exogenous source of hydrogen, which reduces the rate of thermal decomposition, promotes thermal cracking, and inhibits carbon-carbon bond cross linking. The distribution of generated *n*-alkanes is characteristic of a free radical mechanism, with a broad carbon-number distribution (i.e., C₅ to C₃₅) and only minor branched alkanes from known biological precursors (i.e., pristane and phytane). The generation of excess oxygen in the form of CO₂ in hydrous experiments and the high degree of hydrocarbon deuteration in a D₂O experiment indicate that water dissolved in the bitumen is an exogenous source of hydrogen. The lack of an effect on product composition and yield with an increase in H⁺ activity by five orders of magnitude in a hydrous experiment indicates that an ionic mechanism for water interactions with thermally decomposing bitumen is not likely. Several mechanistically simple and thermodynamically favorable reactions that are consistent with the available experimental data are envisaged for the generation of exogenous hydrogen and excess oxygen as CO₂. One reaction series involves water oxidizing existing carbonyl groups to form hydrogen and carboxyl groups, with the latter forming CO₂ by decarboxylation with increasing thermal stress. Another reaction series involves either hydrogen or oxygen in dissolved water molecules directly interacting with unpaired electrons to form a hydrogen-terminated free-radical site or an oxygenated functional group, respectively. The latter is expected to be susceptible to oxidation by other dissolved water molecules to generate additional hydrogen and CO₂. In addition to water acting as an exogenous source of hydrogen, it is also essential to the generation of an expelled saturate-enriched oil that is similar to natural crude oil. This role of water is demonstrated by the lack of an expelled oil in an experiment where a liquid Ga-In alloy is substituted for liquid water. Experiments conducted with high salinity water and high water/rock ratios indicate that selective aqueous solubility of hydrocarbons is not responsible for the expelled oil generated in hydrous pyrolysis experiments. Similarly, a hydrous pyrolysis experiment conducted with isolated kerogen indicates that expelled oil in hydrous pyrolysis is not the result of preferential sorption of polar organic components by the mineral matrix of a source rock. It is envisaged that dissolved water in the bitumen network of a source rock causes an immiscible saturate-enriched oil to become immiscible with the thermally decomposing polar-enriched bitumen. The overall geochemical implication of these results is that it is essential to consider the role of water in experimental studies designed to understand natural rates of petroleum generation, expulsion mechanisms of primary migration, thermal stability of crude oil, reaction kinetics of biomarker transformations, and thermal maturity indicators in sedimentary basins. Copyright © 1997 Elsevier Science Ltd

1. INTRODUCTION

Within the crust of the earth, water is ubiquitous in rock pores, fractures, and hydrated minerals. This ubiquity was demonstrated by the German continental drilling project (KTB), where an abundance of brine waters flowed into the borehole from fractures in hard basement rock at depths greater than 8 km (Kerr, 1994). Less dramatic evidence for the wide-ranging presence of water in the earth's crust stems from its essential role in geological processes spanning a wide range of temperature and pressure conditions from rock weathering (Drever, 1984) at the surface to regional metamorphism (Ferry 1983) and magma generation (Wyllie,

1977) deep within the crust. Intermediate to these extreme conditions, water plays a particularly important role in the subsurface of sedimentary basins as a reactant and transport media for a multitude of inorganic diagenetic reactions including pervasive dolomitization (Machel and Mountjoy, 1987), silica transformations (Williams and Crerar, 1985), smectite illitization (Whitney, 1990), cement/porosity formation (Loucks et al., 1984), and stratabound ore deposition (Garven et al., 1993).

Despite the importance of water and its ubiquity in sedimentary basins, the notion that oil and water do not mix appears to have encouraged organic geochemists to neglect its significance in petroleum formation. This neglect is surprising when

one considers early reports that water vapor reduced the rate of oil generation in oil-shale retorts (Gavin, 1922) and water fluid enhanced the soluble yield from heated coals by an order of magnitude (Fischer, 1925). Jurg and Eisma (1964) were the first to suggest that water had a role in natural petroleum generation. They based this conclusion on differences in the products of thermal decomposition of behenic acid in the presence and absence of liquid water with bentonite clay at temperatures from 200° to 275°C. Low-molecular-weight hydrocarbons generated in the presence of water were indicative of a free-radical mechanism, with *n*-alkanes predominating over isoalkanes as observed in natural crude oils. Conversely, low-molecular-weight hydrocarbons generated in the absence of water were indicative of a carbonium-ion mechanism with isoalkanes predominating over *n*-alkanes. Experiments by Hesp and Rigby (1973) went one step further by showing that the destruction of crude oil to gas was significantly inhibited by the presence of water.

Lewan et al. (1979) reported that heating organic-rich rocks at 330°C for 72 h in the presence of liquid water resulted in generation and expulsion of a petroleum-like oil. This expelled oil is similar to natural crude oils and accumulates on the water surface above the submerged rock within the reactor. The significance of this type of pyrolysis is the expulsion of oil from an organic-rich rock without employing methods that are not operative in the natural system (i.e., organic solvent refluxing, cryogenic trapping, or carrier gas flushing). This type of pyrolysis is referred to as hydrous pyrolysis, and by definition requires liquid water, not H₂O vapor or supercritical fluid, to be in contact with the heated sample (Lewan, 1993a).

Although hydrous pyrolysis has provided information on stages of petroleum formation (Lewan, 1985), kinetics of oil generation (Hunt et al., 1991), maturation of organic-carbon isotopes (Lewan, 1983), biomarker transformations (Peters et al., 1990; Lewan et al., 1986), thermal maturation indices (Lewan, 1985), primary migration and expulsion of oil (Lewan, 1987), and oil generation from coal (Kuangzong et al., 1994; Teerman and Hwang, 1991), the role of water in petroleum formation remains uncertain. In an effort to evaluate the role of water, Hoering (1984) conducted a series of hydrous pyrolysis experiments with pulverized rock, model compounds, and D₂O. This study clearly demonstrated that deuterium exchanged with hydrogen in hydrocarbons that were cleaved from decomposing kerogen, but the specific role of water in the pyrolysis reactions and its ability to promote oil expulsion from an organic-rich rock was not determined. The objective of this study is to address this uncertainty through a series of experiments designed to evaluate various roles water may play in petroleum formation. The experiments compare hydrous pyrolysis with anhydrous pyrolysis, confined-pressure anhydrous pyrolysis, liquid-metal anhydrous pyrolysis, and hydrous pyrolysis experiments using saline water, D₂O, molecular hydrogen, low-pH water, and isolated kerogen.

2. METHODS

2.1. Sample Description

The sample used in these experiments is from a road cut on Interstate Highway I-35 through the Woodford Shale on the south

flank of the Arbuckle Anticline in Carter County, Oklahoma. Woodford Shale is of Devonian-Mississippian age, and at this locality it is thermally immature in the pre-oil generation stage (Lewan, 1987). A fresh unweathered sample was collected from a 14-cm thick bed 3.4 m below the upper contact with an overlying greenish-gray shale. The collected sample is a quartzose claystone with an organic carbon content of 22.39 wt% and an extractable bitumen content of 0.85 wt%. Spherical phosphate concretions measuring 2 to 3 cm in diameter are common in the sampled bed and contain 5.9 weight percent organic carbon. These concretions were easily removed by hand at the outcrop to insure a homogenous shale sample. The sample was crushed into gravel-sized chips (0.5 to 2.0 cm), thoroughly mixed, and designated as WD-26. Amorphous Type-II kerogen accounts for more than 95 volume percent (vol%) of the organic matter in this sample. The kerogen has an atomic H/C ratio of 1.12 and an atomic O/C ratio of 0.10. Seventy-five reflectance measurements on vitrinite macerals found dispersed in the amorphous kerogen gave a mean %Ro of 0.41 with a standard deviation of ±0.05. Rock-Eval pyrolysis of the original rock sample yielded 0.55 wt% volatile hydrocarbons (i.e., S₁ peak), 11.69 wt% generated hydrocarbons (i.e., S₂ peak), and a T-max of 423°C.

2.2. Experimental Conditions

All of the experiments were conducted in stainless-steel 316 or Hastelloy C-276 reactors with carburized surfaces as advised by Lewan (1993a). Table 1 gives the conditions of the experiments used in this study. After the reactors are sealed, they are filled with at least 6.9 MPa of He and leak checked with a thermal-conductivity leak detector before employing the designated head-space medium given in Table 1. The initial vacuum (1–2 kPa) on anhydrous experiments 2, 4, 6, and 8 was established with a drive-belt vacuum pump after the loaded reactor was leak checked with 6.9 MPa of He. Temperatures were monitored with type J thermocouples that were calibrated against national standards at 300, 330, and 360°C. Experiments containing a liquid phase at experimental temperatures typically had a standard deviation less than 0.5°C, and experiments containing only a gas phase at experimental temperatures typically had a standard deviation less than 1.5°C.

The high confining pressure generated from the pyrolysis gases in anhydrous experiment 8 was obtained by pressing 500 g of crushed rock into a 543-cm³ reactor with a hydraulic press. Purity of the D₂O used in experiment 13 was 99.8 wt% deuterium, and 176 g rather than 160 g were used to compensate for its density difference with H₂O. The liquid metal used in experiment 14 is a gallium alloy containing 24.5 wt% indium, which has a high wettability, low melting point (15.7°C), high boiling point (>2000°C), and negligible thermal expansion below 400°C. Using a calculated density of 6.253 g/cm³ for the liquid metal, it was determined that an initial He pressure of 1138 kPa was needed in the head space to obtain a pressure of at least 10 MPa at 330°C. A nickel/chromium screen was fitted over the sample within the reactor to keep the rock submerged in the liquid metal throughout the experiment. All of the hydrous experiments use deionized ASTM type-I water. This quality of water was also used as the source of steam in experiment 9 and to mix the 5 wt% NaCl solution used in experiment 15. The 0.1 N HCl solution used in experiment 16 was analytical grade, with a reported normality range from 0.0999 to 0.1001.

The kerogen used in experiment 18 was isolated from sample WD-26 by methods described elsewhere by Lewan (1986). This isolated organic matter is slightly hydrophobic, which makes it difficult to submerge in the water at the start of the experiment. Prior to loading the reactor, the 40 g of kerogen used in the experiment were mixed with 30 g of isopropyl alcohol, which made the kerogen hydrophilic. The isopropyl alcohol was then removed by filtering 1.2 L of deionized water through the kerogen. The water-wet kerogen and additional water were then added to the reactor, where the kerogen sank to the bottom of the reactor.

2.3. Collection Procedure

After the experiments cooled to room temperature, pressure and temperature were recorded and a sample of head-space gas was

Table 1. Experimental conditions under which rock chips (0.5–2.0 cm) of Woodford Shale (WD-26) were pyrolyzed.

Experiment no.	Temperature (°C)	Duration (h)	Median employed ^a (gas [kPa]/liquid [g])	Rock (g)	Reactor ^b (cm ³ /S-H)	Final pressure ^c (MPa)
1	300.4	72.00	He[241]/H ₂ O[320]	400.0	1000/S	9.76
2	300.1	72.00	Vacuum/anhydrous	400.0	1000/S	2.17
3	329.7	72.00	He[241]/H ₂ O[320]	400.0	1000/S	15.89
4	330.0	72.00	Vacuum/anhydrous	400.0	1000/S	4.24
5	350.3	72.00	He[241]/H ₂ O[320]	400.0	1000/S	21.13
6	350.6	72.00	Vacuum/anhydrous	400.0	1000/S	5.69
7	350.5	72.00	He[7722]/anhydrous	400.0	1000/S	23.48
8	349.7	72.00	Vacuum/anhydrous	500.1	534/S	21.76
9	350.6	72.00	He[241]/H ₂ O[75]	400.0	1000/S	18.31
10	330.0	70.70	He[241]/H ₂ O[160]	200.0	534/H	15.48
11	329.7	70.70	He[241]/H ₂ O[160]	200.0	534/H	15.34
12	329.9	70.85	He[241]/H ₂ O[450]	200.0	1000/H	14.17
13	330.1	70.57	He[241]/D ₂ O[176]	200.0	534/H	15.69
14	330.0	70.60	He[1138]/Ga-In[1507]	200.0	534/H	10.31
15	329.9	70.55	He[241]/5% NaCl[160]	200.0	534/H	16.17
16	329.5	70.70	He[241]/0.1 N HCl[160]	200.0	534/H	15.79
17	327.6	70.70	H ₂ [1482]/H ₂ O[160]	200.0	534/H	13.93
18	330.0	72.00	He[241]/H ₂ O[254]	40.0 ^d	534/H	14.86

^a Media refers to headspace gas in reactor and liquid in contact with crushed rock.

^b S = stainless-steel 316 and H = Hastelloy C-276.

^c Pressure in reactor at experimental temperature at the end of the experiment.

^d Sample is isolated kerogen from sample WD-26.

collected in an evacuated 30-cm³ stainless-steel cylinder. Expelled oil generated in the hydrous pyrolysis experiments was collected in three steps. First, the majority of expelled oil was collected from the surface of the water in the reactor with a Pasteur pipet. Second, the water and minor amounts of expelled oil not collected with the pipet were decanted into a glass separatory funnel. The separated oil was concentrated at the stop cock of the funnel, where it was collected with the same Pasteur pipet used to collect the oil on the water surface. Third, the thin film of expelled oil on the reactor walls, separatory funnel, Pasteur pipet, and rock chips was rinsed with benzene at room temperature. This benzene rinse was filtered through a 0.45 μ m polytetrafluoroethylene (PTFE) filter and the expelled oil was concentrated by rotary vacuum evaporation of the benzene. The isolated kerogen in experiment 18 did not include a benzene rinse of the remaining bitumen-kerogen mixture or the reactor walls below the water surface. The decanted water was filtered through a 0.45 μ m cellulose-acetate/nitrate filter. Immediately following its filtration, the pH was determined with pH and single-junction reference electrodes and the Eh was determined with a platinum redox combination electrode. Electrode responses were measured on a Orion 901 benchtop meter. Rock chips were removed from the reactor and dried in a vacuum oven at 50°C for 24 h. The dried rock chips were pulverized and bitumen was extracted in a Soxhlet apparatus for 72 h with an azeotropic mixture of benzene and methanol (60:40 wt%). The refluxed solvent was filtered through a 0.45 μ m PTFE filter and the bitumen was concentrated by rotary vacuum evaporation. Rock chips recovered from the liquid metal in experiment 14 contained patches of the metal alloy on their surfaces that could not be removed. In order to correct for this additional weight in the bitumen extraction, an aliquot of the pulverized rock chips was analyzed for Ga and In by ICP/mass spectrometry within a detection limit of 1 ppm (X-ray Assay Laboratories). Based on these analyses, the amount of bitumen extracted from this rock was corrected for the addition of 81,200 ppm of Ga and 25,500 ppm of In sorbed on the rock.

2.4. Pyrolysate Analyses

Gas compositions were determined on a CEC103 mass spectrometer using an enhanced version of the ASTM D2650-88 method to determine mole percentages, which were converted to mole concentrations assuming ideal gas behavior at room temperatures. Anhydrous experiments generated no expelled oil, but generated a bitumen

within the rock chips. In order to compare the pyrolysates from hydrous and anhydrous experiments in an equitable manner, a proportionally representative composite of bitumen and expelled oil from hydrous experiments 1, 3, and 5 was prepared for gas chromatography/mass spectrometry (GC/MS) comparisons with the bitumen from anhydrous experiments 2, 4, and 6. This mixture of expelled oil and bitumen is based on the weight percent yields given in Table 2 and is referred to as composited pyrolysate to distinguish it from the bitumen of anhydrous experiments. Compositional differences between expelled oil and bitumen from hydrous experiments have been demonstrated (Lewan, 1983; Lewan et al., 1986; Peters et al., 1990), but in this study they were combined to facilitate an easier comparison with anhydrous experiments. Composited pyrolysates and bitumens were separated on a 40-cm alumina (MCB Alcoa F-20) column. The saturate fraction was eluted with 275 mL of *n*-heptane, the aromatic fraction was eluted with 275 mL of benzene, and the polar (NSO) fraction was eluted with an equal volume mixture of benzene and methanol. Eluting solvents and light hydrocarbons (i.e., C₆–C₁₃) are removed by rotary vacuum evaporation. Saturate and aromatic fractions were analyzed on a Hewlett-Packard 5996A GC/MS. Instrument conditions and operation are discussed elsewhere by Lewan et al. (1986).

2.5. Kerogen Analyses

Kerogen was isolated from pulverized rock chips by a series of HCl and HF treatments followed by a heavy-liquid separation. Specifics on this procedure are given by Lewan (1986). Elemental analyses of isolated kerogen include carbon, hydrogen, nitrogen, and oxygen. Determinations were made on a Carlo Erba 1106 elemental analyzer with acetanilide as the standard for C, H, and N, and benzoic acid as the standard for oxygen. Stable carbon isotopes ($\delta^{13}\text{C}$) of the isolated kerogens were determined relative to the PDB standard as described by Lewan (1983). Vitrinite reflectance measurements were made on polished slides of isolated kerogens as described by Buchardt and Lewan (1990). The ratio of aromatic ring carbons to total carbons (f_a) was determined by NMR on the isolated kerogens by Spectral Data Services.

3. EXPERIMENTAL RATIONALE AND RESULTS

3.1. Hydrous Versus Anhydrous

Gas, expelled oil, bitumen, and total pyrolysate (i.e., gas + expelled oil + bitumen) yields are given in Table 2 for

Table 2. Types and amounts (wt% rock) of pyrolysates generated in hydrous and anhydrous experiment.

Temp./Time	300°C/72 h		330°C/72 h		350°C/72 h	
	hydrous Experiment no. 1	anhydrous Experiment no. 2	hydrous Experiment no. 3	anhydrous Experiment no. 4	hydrous Experiment no. 5	anhydrous Experiment no. 6
Bitumen Extract	8.35	8.66	8.19	6.62	5.71	3.30
Expelled Oil	0.65	0.00	2.79	0.00	4.15	0.00
Generated Gas	0.43	0.78	1.05	1.74	1.68	2.40
Total Pyrolysate	9.43	9.44	12.03	8.36	11.54	5.70

72-h hydrous and anhydrous experiments at 300, 330, and 350°C (experiments 1 through 6). Lack of an expelled oil and greater amounts of gas in anhydrous experiments relative to hydrous experiments are the most obvious differences in yields. In addition, total pyrolysate yields of the hydrous experiments gradually exceed those of the anhydrous experiments with increasing temperature. Total pyrolysate yields for the hydrous and anhydrous experiments are essentially the same after 72 h at 300°C (experiments 1 and 2), which represent conditions under which kerogen decomposes to bitumen (Lewan, 1983, 1985). The similar amounts (Table 2) and compositional character (Table 5) of the bitumens suggest that bitumen generation is not significantly influenced by the presence of water. However, the more generated hydrocarbon gas (Table 2), reduced whole-rock S_2 peak (Table 3), lower kerogen atomic H/C ratio (Table 4), and higher kerogen NMR aromaticity index (Table 4) under anhydrous conditions indicate that the residual kerogen may be influenced by the presence of water. The bitumen content decreases at the higher temperatures under hydrous and anhydrous conditions, but the bitumen decrease is greater under anhydrous conditions with no expelled oil or significant quantity of generated gas to account for this decrease. The amount of expelled oil increases in the hydrous experiments from 330 to 350°C as the bitumen content decreases. These differences at 330 and 350°C indicate that bitumen decomposition results in oil generation under hydrous conditions and insoluble-bitumen (i.e., pyrobitumen) generation under anhydrous conditions. At 350°C after 72 h, the total pyrolysate yield under hydrous conditions is twofold greater than the total pyrolysate yield under anhydrous conditions.

Rock-Eval pyrolysis data also shows significant differences between hydrous and anhydrous experiments (Table 3). Volatile hydrocarbons denoted by the S_1 peak decrease under anhydrous conditions from 2.31 to 1.67 wt% of rock with increasing experimental temperature. Conversely, the S_1 -peak hydrocarbons increase under hydrous conditions from 1.81 to 2.57 wt% of rock with increasing experimental temperature. Generated hydrocarbons denoted by the S_2 peak decrease with increasing temperature for hydrous and anhydrous experiments, but the values are consistently lower under anhydrous conditions. The hydrous to anhydrous ratio of the S_2 peak increases from 1.37 at 300°C to 3.79 at 350°C after 72 h. These results support the observation that anhydrous conditions reduce the hydrocarbon yield of a rock relative to hydrous conditions. Production indices (i.e., $S_1/[S_1 + S_2]$) increase under both conditions, but are consistently higher in the anhydrous experiments. As an oil-genera-

tion index, this ratio suggests that oil generation occurs at a lower thermal stress under anhydrous conditions than under hydrous conditions. This observation is supported in part by the higher T -max value for the anhydrous experiment at 330°C. Another important difference between hydrous and anhydrous conditions is the amount of hydrocarbons expelled from the recovered pyrolyzed rocks as calculated from the Rock-Eval data by the method proposed by Cooles et al. (1986). Lewan et al. (1995) have previously shown that this method overestimates the amounts of hydrocarbon expelled from rocks subjected to hydrous pyrolysis by more than a factor of two. Similarly, the calculated values for the hydrous pyrolysis experiments at 330 and 350°C for 72 h in Table 3 (experiments 3 and 5) also give exaggerated amounts of calculated expelled hydrocarbon compared with the measured amounts of total expelled pyrolysates. However, the amount of exaggeration between hydrous and anhydrous pyrolysis is significantly different, with anhydrous pyrolysis yielding calculated amounts of expelled oil that are 6 to more than 7 times greater than the actual amounts of total expelled pyrolysate (Table 3).

Results from various analyses conducted on kerogens isolated from rocks recovered from the hydrous and anhydrous experiments are given in Table 4. The stable carbon isotopes of kerogens in both hydrous and anhydrous experiments show a slight depletion in ^{12}C with increasing thermal stress. As noted by Lewan (1983), this isotopic shift is not significant and is typically within the analytical error for kerogen determinations. No significant difference occurs in this isotopic shift between the hydrous and anhydrous experiments. Similarly, atomic N/C, O/C, and Org S/C ratios from the elemental analyses of the isolated kerogens show no significant differences between hydrous and anhydrous experiments (Table 4). However, the atomic H/C ratio is consistently lower under anhydrous conditions. This difference suggests that kerogens pyrolyzed under anhydrous conditions develop a more aromatic and condensed structure than kerogens pyrolyzed under hydrous conditions. Solid state ^{13}C -NMR spectra also showed a significantly higher carbon aromaticity (f_a) for the isolated kerogens pyrolyzed under anhydrous conditions (Table 4). Reflectance measurements made on minor to trace amounts of vitrinite dispersed within the predominantly amorphous kerogen gave consistently higher mean reflectance values under anhydrous conditions (Table 4). Although these vitrinite reflectance values are suppressed (Lewan, 1993b), they support the findings from the NMR data and atomic H/C ratios that kerogen aromatizes and condenses more readily under anhydrous conditions

Table 3. Total organic carbon (TOC) and Rock-Eval pyrolysis data on recovered rock from hydrous and anhydrous experiments.

Temp./Time	300°C/72 h		330°C/72 h		350°C/72 h	
	hydrous Experiment no.	anhydrous 2	hydrous 3	anhydrous 4	hydrous 5	anhydrous 6
TOC (wt% rock)	21.53	21.33	19.44	19.79	17.75	19.54
S ₁ -Peak (wt% rock)	1.81	2.31	2.27	2.17	2.57	1.67
S ₂ -Peak (wt% rock)	10.46	7.61	3.23	1.65	1.48	0.39
S ₁ /(S ₁ + S ₂)	0.15	0.23	0.41	0.57	0.63	0.81
T-Max (°C)	439	440	444	466	408	411
Calculated expelled hydrocarbons (wt% rock)	-1.05	3.13	9.43	12.92	10.42	15.93
Measured expelled oil and gas ^b (wt% rock)	1.08	0.78	3.84	1.74	5.83	2.40

^a Based on method described by Cooles et al. (1986) using an inert carbon fraction of 0.538 from Rock-Eval data on the original unheated sample.

^b Sum of expelled oil and generated gas given in Table 2.

than under hydrous conditions at the same experimental thermal stress levels.

GC/MS parameters measured on the bitumen from the anhydrous experiments, and the composited pyrolysate from the hydrous experiments show the former to be at a higher thermal maturity than the latter at the same level of thermal stress (Table 5). The *m/z* 57 ion chromatograms (Fig. 1) show the anhydrous bitumens have a more condensate-like-*n*-alkane distribution (*n*C₁₅/*n*C₂₅, Table 5) and a more rapid reduction in acyclic isoprenoids relative to *n*-alkanes (*n*C₁₇/Pristane, Table 5) than the hydrous composited pyrolysates. Similarly, biomarker indices also show higher levels of thermal maturity under anhydrous conditions. The triaromatic

steroid cracking index reaches its maximum of 1.00 at 330°C after 72 h under anhydrous pyrolysis, and at 350°C after 72 h under hydrous pyrolysis (TAS-Index, Table 5; Fig. 2). Similarly, phenanthrene indices (MPI-1 and MPR, Table 5; Fig. 3) and terpane indices (TT-Index and TPT-Index, Table 5; Fig. 4) consistently indicate higher maturity levels in the anhydrous bitumens relative to the hydrous composited pyrolysates. These higher maturities in the anhydrous bitumens are also reflected in the relative abundances of biomarkers. Steranes in the *m/z* 217 ion chromatograms after 72 h at 330°C are indistinguishable from background noise under anhydrous conditions (Fig. 5e), but are distinguishable under hydrous conditions (Fig. 5b). Similarly, mono-

Table 4. Analyses of kerogens isolated from rocks after hydrous and anhydrous experiments.

Temp./time	300°C/72 h		330°C/72 h		350°C/72 h	
	hydrous Experiment no.	anhydrous 2	hydrous 3	anhydrous 4	hydrous 5	anhydrous 6
Kerogen Carbon ^a (wt% ext. rock)	17.67	17.23	14.96	16.38	15.05	17.53
Elemental analyses (wt% kerogen)						
Carbon	75.1	75.8	77.4	78.3	78.8	79.5
Hydrogen	6.2	5.7	4.7	4.1	3.9	3.8
Nitrogen	2.9	3.2	3.7	3.9	4.0	3.9
Oxygen	9.3	8.9	8.2	8.0	8.1	8.0
Org. Sulfur ^b	6.5	6.5	6.0	5.7	5.2	4.8
Atomic Ratios						
H/C	0.99	0.90	0.72	0.64	0.60	0.57
N/C	0.03	0.04	0.04	0.04	0.04	0.04
O/C	0.09	0.09	0.08	0.08	0.08	0.08
Org. S/C	0.03	0.03	0.03	0.03	0.02	0.02
Aromaticity (NMR-Ca)	0.31	0.45	0.53	0.65	0.69	0.82
Vitrinite (% R ₀)	0.60	0.65	0.72	1.02	1.22	1.51
δ ¹³ C (‰ vs PDB)	-31.5	-31.3	-30.7	-30.6	-30.5	-30.5

^a Organic carbon of recovered rock after bitumen extraction.

^b Determined from total iron and total sulfur analyses on the basis of organic S = total S - (total Fe × 1.148).

Table 5. Molecular GC/MS ratios of total pyrolysates from hydrous and anhydrous experiments.

Temp./time	300°C/72 h		330°C/72 h		350°C/72 h	
	hydrous Experiment no. 1	anhydrous 2	hydrous 3	anhydrous 4	hydrous 5	anhydrous 6
nC_{15}/nC_{25}^a	7.62	8.10	6.58	8.58	7.14	11.50
Pristane/phytane ^a	1.88	2.03	1.79	1.86	1.77	2.00
$nC_{17}/Pristane^a$	1.81	2.33	3.09	5.00	5.36	8.71
TAS-Index ^b	0.38	0.52	0.74	1.00	1.00	1.00
MPI-1 ^c	0.77	0.82	0.84	0.96	0.93	0.97
MPR ^d	0.87	0.93	0.96	1.14	1.00	1.24
TT-Index ^e	0.25	0.37	0.42	0.60	0.70	1.00
TPT-Index ^f	0.13	0.15	0.34	0.63	1.00	PBDL

^a Ratio calculated from peak heights on the m/z 57 ion chromatograms with pris. = pristane and phy. = phytane.

^b Triaromatic steroid index = $(C_{20} + C_{21})/C_{20} + C_{21} + C_{26} + C_{27} + C_{28}$ peak heights from the m/z 231 ion chromatograms.

^c Methyl phenanthrene index = $1.5(2MP + 3MP)/(P + IMP - 9MP)$ peak heights from the m/z 178 + 192 composite ion chromatograms.

^d Methyl phenanthrene ratio = $2MP/IMP$ peak heights from the m/z 192 ion chromatogram.

^e Tricyclic terpene index = $C_{19}/(C_{19} + C_{23})$ peak heights from the m/z 191 ion chromatogram.

^f Tricyclic/pentacyclic terpene-index = $C_{19}/(C_{19} + C_{30})$ peak heights from the m/z 191 ion chromatograms. PBDL = peaks below detection limit.

aromatic steroids in the m/z 253 ion chromatograms (Fig. 6) after 72 h at 330°C are dwarfed by n -alkanes under anhydrous conditions (Fig. 6e), but distinguishable under hydrous conditions (Fig. 6b). Although dilution of these biomarkers by increased pyrolysate yields (Table 2) may account for some of their apparent degradation in the hydrous experiments, the decreasing pyrolysate yields (Table 2) in the anhydrous experiments indicates thermal degradation predominates over dilution. The pristane/phytane ratio, which is commonly used to evaluate organic-source input of source rocks (Peters and Moldowan, 1993), is the only measured parameter that does not change significantly with thermal stress or pyrolysis conditions.

Compositions of head-space gas generated during the hydrous and anhydrous experiments are given in Table 6. Anhydrous experiments consistently have more hydrocarbon gases, molecular hydrogen, and hydrogen sulfide than hydrous experiments. Conversely, hydrous experiments consistently have more carbon dioxide than anhydrous experiments. Methane content in both hydrous and anhydrous experiments consists of approximately 50 mol% of the hydrocarbon gases, which is significantly lower than that observed in natural gas as discussed by Tannenbaum and Kaplan (1985). C_2 through C_4 alkenes are present in trace quantities in both hydrous and anhydrous experiments, but their variability shows no correlation with experimental conditions. Except for the hydrous experiment at 330°C (experiment 3), which had no detectable C_2 through C_4 alkenes, propene is the most dominant of these three alkenes in both the hydrous and anhydrous experiments. Concentrations of these three alkenes are higher in the hydrous experiments at 300°C for 72 h, but are lower in the hydrous experiments at 350°C for 72 h. Molecular hydrogen concentrations increase as experimental temperatures increase for both hydrous and anhydrous experiments. However, the molecular hydrogen concentration increases more rapidly under anhydrous condi-

tions, with the anhydrous concentration being almost twice that of the hydrous concentration at 350°C after 72 h (Table 6). These results indicate that more hydrogen is either being generated under anhydrous conditions or consumed under hydrous conditions.

In order to properly compare concentrations of H_2S and CO_2 in hydrous and anhydrous experiments, the amounts of these gases and their related aqueous species dissolved in the water of the hydrous experiments must be determined. Table 7 shows that methane, ethane, and molecular hydrogen have only a minor dissolved aqueous component, whereas CO_2 and H_2S have a dissolved component that typically exceeds their head-space gas concentrations. Total CO_2 (i.e., aqueous species plus gas) is consistently higher in the hydrous experiments than in the anhydrous experiments. This difference at 350°C is more than one order of magnitude. This exceptional amount of CO_2 generated under hydrous conditions at 350°C raises the issue of whether H_2O interacts with organic matter to generate additional oxygen in the form of CO_2 . Mass balance calculations based on the oxygen lost from kerogen during the experiments were made to address this issue. Results in Table 8 show that 307 mmol of oxygen are lost from the original kerogen and that 480 mmol of oxygen are formed as CO_2 after 72 h at 350°C under hydrous conditions. This excess of 173 mmol of oxygen at 350°C after 72 h indicates that an additional source of oxygen is needed. The excess oxygen is a minimum value because additional CO_2 dissolved in bitumen and expelled oil are not included in the calculations. The additional oxygen occurring as CO_2 dissolved in the bitumen and oil of experiment 5 is approximately 8 mmol as determined by the Peng-Robinson equation-of-state (Peng and Robinson, 1976) as facilitated by the EQUI-PHASE program (D. B. Robinson Research, Ltd., Edmonton, Alberta). The additional oxygen occurring in C_2 through C_5 aliphatic monocarboxylic acids dissolved in the surrounding water of experiment 5 is approximately

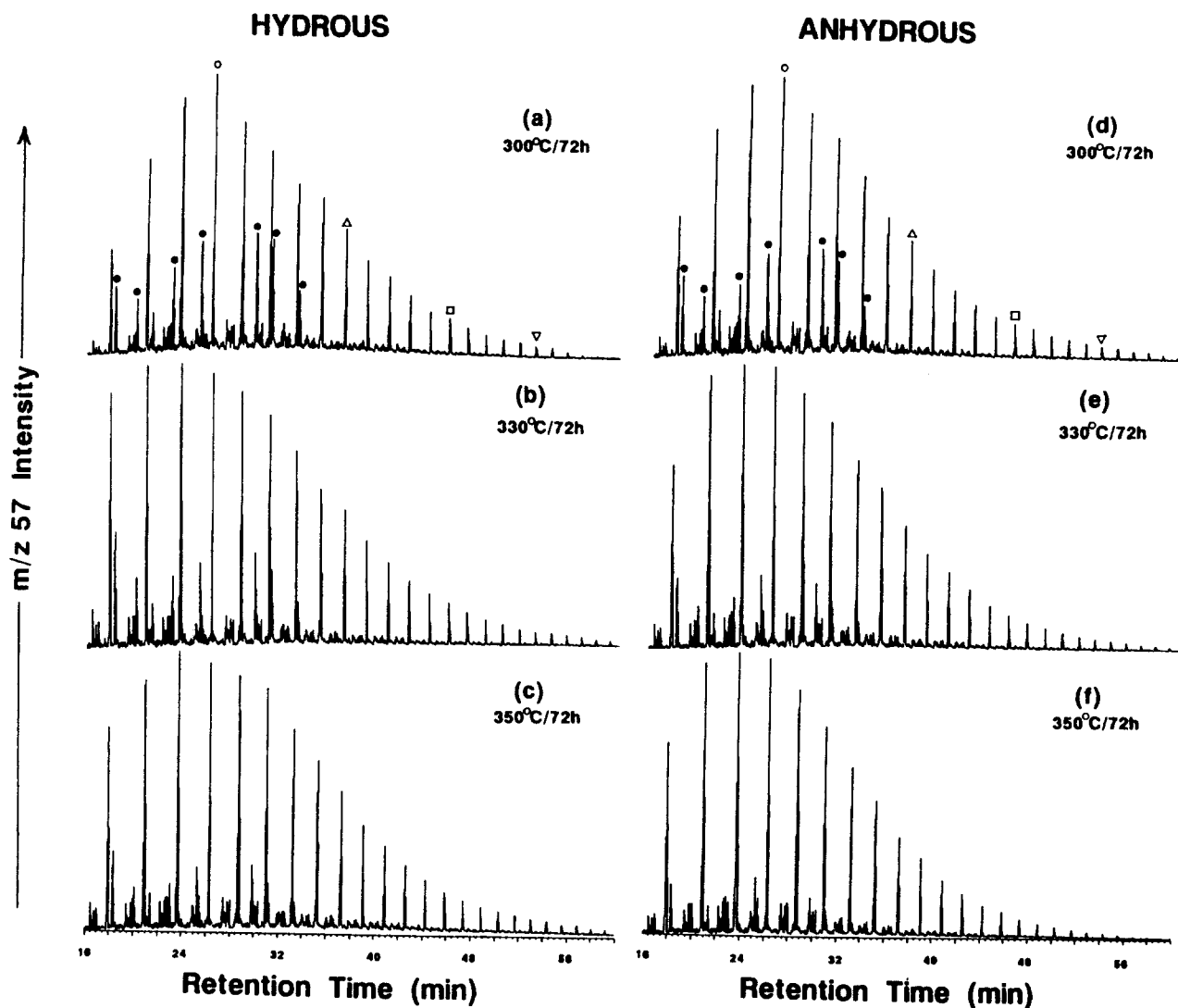


Fig. 1. m/z 57 ion chromatograms of the saturate fraction of the total pyrolysates from hydrous (a, b, and c) and anhydrous (d, e, and f) experiments. Prominent peaks represent normal alkanes with n -C₁₅ denoted by \circ ; n -C₂₀ denoted by Δ ; n -C₂₅ denoted by \square ; and n -C₃₀ denoted by ∇ . Peaks representing acyclic isoprenoids with 13 through 20 carbons are denoted by \bullet , with the exception of the C₁₇-isoprenoid, which is not present.

33 mmol based on maximum acid yields from hydrous pyrolysis of the Phosphoria Retort Shale (Lewan and Fisher, 1994, Table 3). Therefore, the total excess oxygen in the form of CO₂ or aqueous carboxylic acids is approximately 521 mmol. The lack of carbonate minerals in the original rock (i.e., <0.05 wt% carbonate carbon) leaves only H₂O as the source of this excess oxygen.

Except for the experiments at 300°C for 72 h, total H₂S (i.e., aqueous species plus gas) is greater in the hydrous experiments than in the anhydrous experiments. This difference at 350°C is only twofold as compared with the tenfold difference reported for CO₂. A sulfur-mass balance (Table 8) also indicates an excess of sulfur in the form of H₂S relative to the amount of organic sulfur lost from the original kerogen under hydrous conditions at 350°C after 72 h. However, this excess is relatively small and may be explained by dissolution of pyrite exposed to water at the

surface of the rock chips. Similar to the mass balance calculations for oxygen, the amount of S remaining in the kerogen is greater under anhydrous than hydrous conditions at 350°C after 72 h. These results indicate that sulfur, like oxygen, is more readily released from the original organic matter under hydrous conditions than under anhydrous conditions. A nonisothermal pyrolysis study from 300 to 500°C with lignite also shows that more than three times as much sulfur is incorporated into the residual semicoke under a stream of argon than under a stream of water vapor (Minkova et al., 1991).

3.2. Confined Pressure Versus Hydrous

Final pressures at experimental temperatures are higher in the hydrous experiments than in the anhydrous experiments (Table 1). This difference is a result of the hydrous pressures

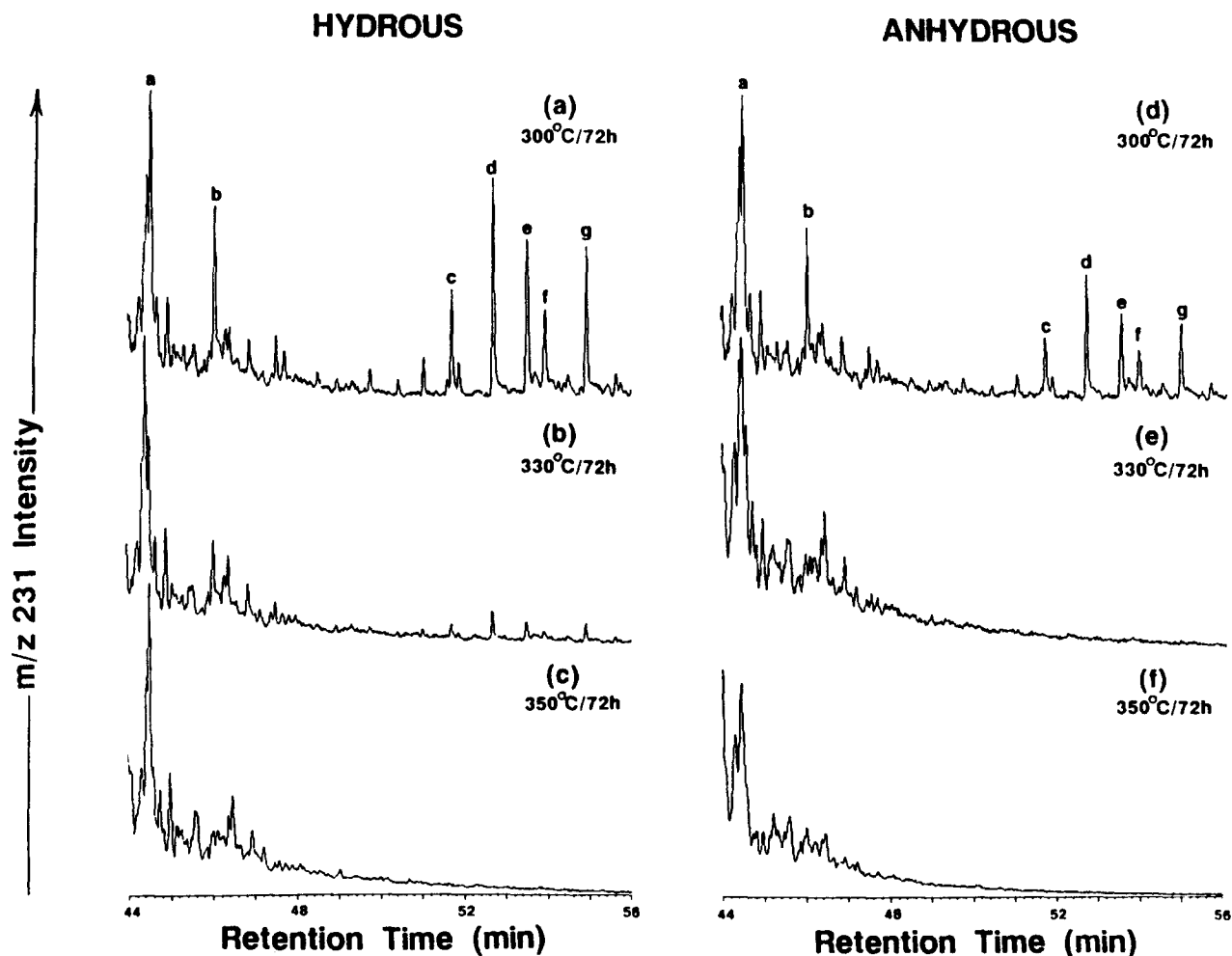


Fig. 2. m/z 231 ion chromatograms of aromatic fraction of the total pyrolysate from hydrous (a, b, and c) and anhydrous (d, e, and f) experiments. The peak designations are in reference to ABC-ring triaromatic steroid hydrocarbons: a = C_{20} ; b = C_{21} ; c = C_{26} (20S); d = C_{26} (20R) plus C_{27} (20S); e = C_{28} (20S); f = C_{27} (20R); and g = C_{28} (20R).

being made up of water vapor, generated gas, and added helium, with the anhydrous pressures only being composed of generated gas. The significance of this pressure difference is examined in three experiments (7, 8, and 9) at 350°C for 72 hours. Experiment 7 is under anhydrous conditions with an initial helium pressure of 7.72 MPa. After 72 h at 350°C, the final pressure is 23.48 MPa of generated gas plus the initially added helium. Table 9 shows that the higher confining pressure results in a slightly lower total pyrolysate yield than that of the low-pressure anhydrous experiment 6. The gas analyses in Table 10 show that with the exception of iso-butane, the amounts of C_1 through C_4 alkanes, carbon dioxide, and hydrogen sulfide are intermediate to those of the hydrous and low-pressure anhydrous experiments 5 and 6, respectively. Molecular hydrogen, ethene, and propene are significantly more abundant, which suggests less interaction between hydrogen and cleaved ethyl and propyl functional groups in the He-pressurized anhydrous (experiment 7). These results indicate that the major differences in types and amounts of yield between hydrous and anhydrous conditions

at 350°C after 72 h (experiments 5 and 6) cannot be attributed to differences in the experimental gas pressures.

Experiment 8 considers the conclusion by Monthieux et al. (1985) that confinement of generated gas in anhydrous experiments produces results similar to those in hydrous experiments. This experiment involves reducing the available gas volume by mechanically pressing 500 g of crushed rock (0.5–1.0 cm; WD-26) into a 534-cm³ reactor, which was then evacuated. After 72 h at 350°C, the pressure of the generated gas was similar to that of the hydrous experiment (experiment 5, Table 9). However, similar to the He-pressured anhydrous experiment 7, the total pyrolysate yield is slightly lower than that of the low-pressure anhydrous experiment 6 and less than that of the hydrous experiment 5 by more than a factor of 2 (Table 9). The generated gases in experiment 8 (Table 10) contain significantly lower concentrations of propene and molecular hydrogen than the hydrous or anhydrous experiments (Table 6, experiments 5 and 6). Relative to the anhydrous experiment 6, the He-pressured anhydrous experiment 7 has greater amounts of propene and

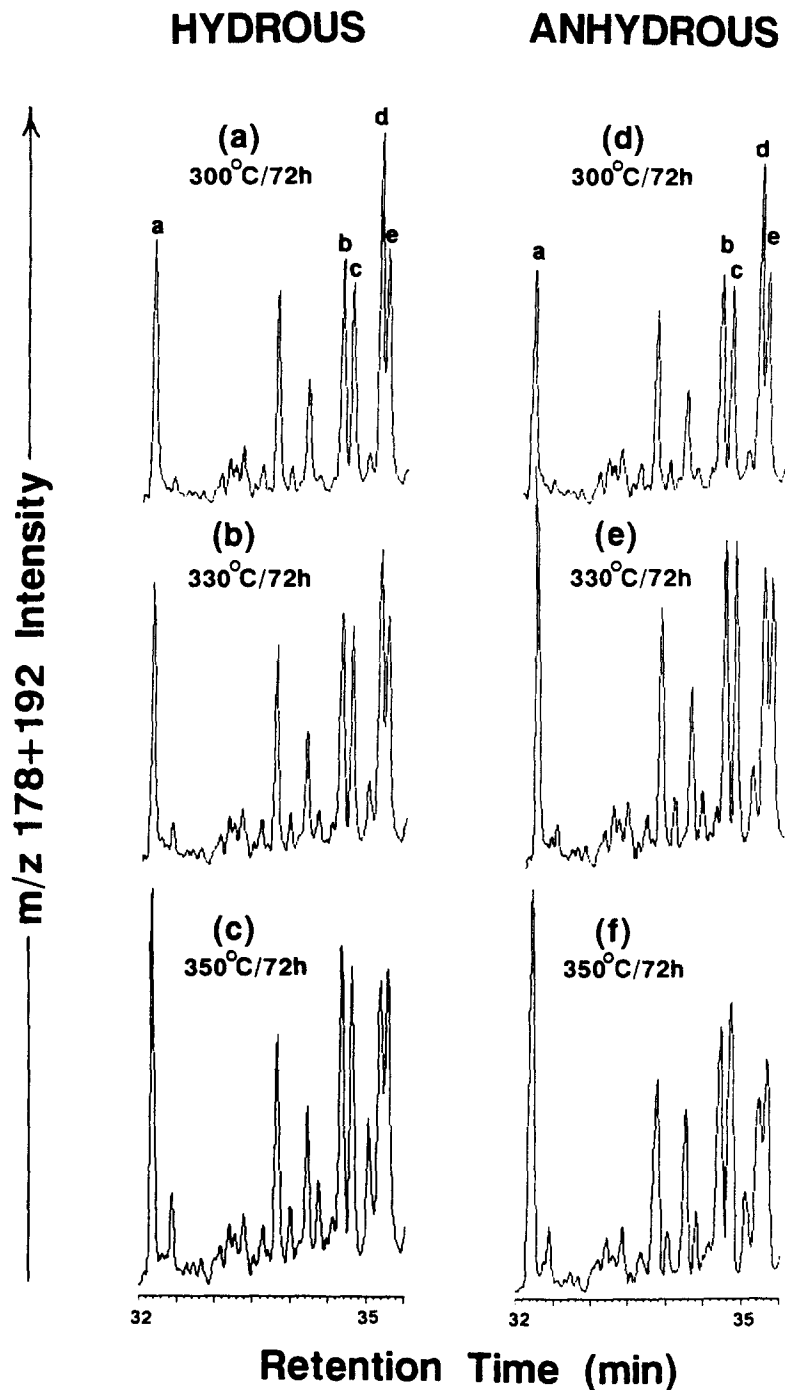


Fig. 3. m/z 178 + 192 composited ion chromatograms of aromatic fraction of the total pyrolysates from hydrous (a, b, and c) and anhydrous (d, e, and f) experiments. The peak designations are a = phenanthrene; b = 3-methyl phenanthrene plus 1-methyl dibenzothiophene; c = 2-methyl phenanthrene; d = 9-methyl phenanthrene; and e = 1-methyl phenanthrene.

molecular hydrogen and a lesser amount of methane. Conversely, the confined-pressure anhydrous experiment 8 has the least amount of alkenes and molecular hydrogen and the greatest amount of methane.

Experiment 9 has a confining pressure comprised of water vapor and generated gas. This experiment is not considered hydrous because of the lack of liquid water in contact with

the rock. The amount of water used in this experiment is sufficient only to generate water vapor, and is therefore referred to as steam pyrolysis. Although no expelled oil was generated in this experiment (Table 9), the total pyrolysate yield is intermediate to that of the hydrous and anhydrous experiments (experiments 5 and 6, respectively). Similarly, nonisothermal pyrolysis experiments from 300 to 500°C with

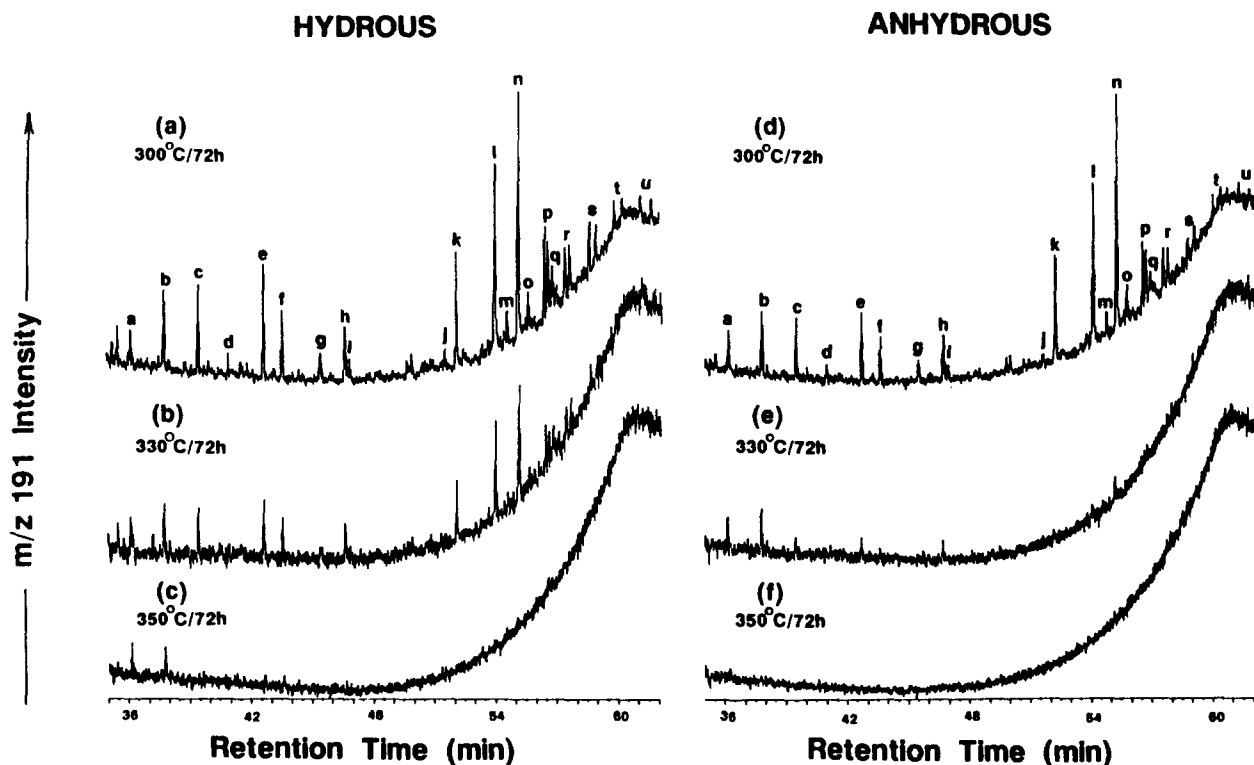


Fig. 4. m/z 191 ion chromatograms of the saturate fraction of the total pyrolysates from hydrous (a, b, and c) and anhydrous (d, e, and f) experiments. The peak designations are a = C_{19} -tricyclic terpene; b = C_{20} -tricyclic terpene; c = C_{21} -tricyclic terpene; d = C_{22} -tricyclic terpene; e = C_{23} -tricyclic terpene; f = C_{24} -tricyclic terpene; g = C_{25} -tricyclic terpene; h = C_{24} -tetracyclic terpene; i = C_{26} -tricyclic terpenes; j = $18\alpha(H)$ -trisorneohopane; k = $17\alpha(H)$ -trisorneohopane; l = $17\alpha(H),21\beta(H)$ -norhopane; m = $17\beta(H),21\alpha(H)$ -norhopane; n = $7\alpha(H),21\beta(H)$ -hopane; o = $17\beta(H),21\alpha(H)$ -hopane; p = $17\alpha(H),21\beta(H)$ -homohopanes S and R at C-20; s = $17\alpha(H),21\beta(H)$ -trishomohopanes S and R at C-20; t = $17\alpha(H),21\beta(H)$ -tetrakishomohopanes S and R at C-20; and u = $17\alpha(H),21\beta(H)$ -pentakishomohopanes S and R at C-20. Peaks j through u will be collectively referred to as pentacyclic terpenes, and peaks p, r, s, t, and u will be collectively referred to as extended hopanes.

lignite, bituminous coal, and oil shale, show liquid product yields are, respectively, 40, 52, and 73 wt% higher under a stream of water vapor than under a stream of argon (Minkova et al., 1991). The amounts of generated C_1 through C_6 alkanes, molecular hydrogen, hydrogen sulfide, and total gas are also intermediate to those of the hydrous and anhydrous experiments as shown in Table 10 (experiments 5 and 6). The CO_2 content of this experiment is higher than that of the hydrous experiment (5), but this difference can be attributed to the lower amounts of aqueous CO_2 in the steam experiment during collection at room temperatures. As shown in Table 7, a considerable amount of CO_2 can be dissolved in the aqueous phase, which is less in the steam experiment by a factor of 4.27 (Table 1). Taking into account this dissolved component, the total CO_2 (i.e., gaseous + aqueous) in the steam experiment also occurs intermediate to the hydrous and anhydrous experiments.

3.3. Water Chemistry

In order to develop an understanding of the role of water in the hydrous pyrolysis, a series of experiments was conducted with different water chemistries (Table 11). Duplicate experiments at $330^\circ C$ for 70.7 h (experiments 10 and

11) with deionized water show the variation in yield one may expect in these experiments (Table 11). Although it has previously been demonstrated that the size of the rock chips have no appreciable effect on the product yield (Lewan, 1993a), no data have been presented on the effect of water/rock ratios on the amount of product yield under hydrous conditions. Experiment 12 has a water/rock ratio 2.8 times greater than the water/rock ratio of 0.8 used in experiments 10 and 11. As shown in Table 11, this difference does not have a significant effect on the yields of expelled oil and generated gas. The lower gas yield relative to experiments 10 and 11 may be attributed to more gas being dissolved in the greater mass of water used in experiment 12. It is also noteworthy that although these experiments are scaled down from experiment 3 by a factor of 2, they have similar expelled-oil yields. The slightly higher yields in experiment 3 may be attributed to its longer duration (Table 1). Higher gas yields in experiments 10, 11, and 12 relative to experiment 3 are most likely the result of improved head-space volume and pressure determinations developed over the 2-year period between experiment 3 and the other experiments (10, 11, and 12).

The importance of hydrogen as H^+ and H_2 under hydrous conditions is examined in experiments 16 and 17, respec-

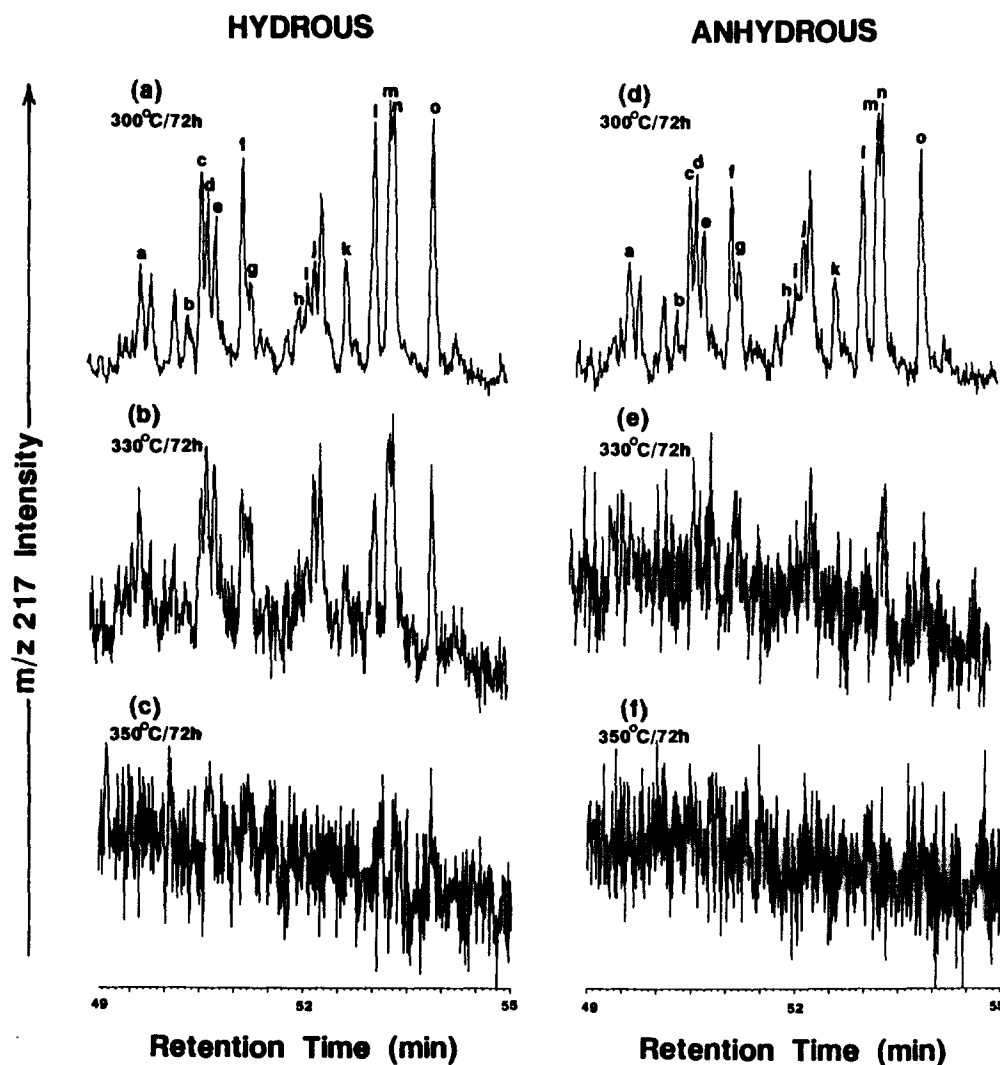


Fig. 5. m/z 217 ion chromatograms of the saturate fraction of the total pyrolysates from hydrous (a, b, and c) and anhydrous (d, e, and f) experiments. The peak designations are a = 24-methyl-13 β (H),17 α (H)-diacholestane (20S); b = 24-methyl-13 β (H),17 α (H)-diacholestane (20R); c = 14 α (H),17 α (H)-cholestane (20S) plus possible coelution of a 24-methyl-diacholestane; d = 14 β (H),17 β (H)-cholestane (20R) plus possible coelution of a 24-methyl-diacholestane; e = 14 β (H),17 β (H)-cholestane (20S) plus possible coelution of a 24-methyl-diacholestane; f = 14 α (H),17 α (H)-cholestane (20R); g = 24-ethyl-13 β (H),17 α (H)-diacholestane (20R); h = 24-methyl-14 α (H),17 α (H)-cholestane (20S); i = 24-methyl-14 β (H),17 β (H)-cholestane (20R) plus possible coelution of 24-ethyl-13 α (H),17 β (H)-diacholestane (20R); j = 24-methyl-14 β (H),17 β (H)-cholestane (20S); k = 24-methyl-14 α (H),17 α (H)-cholestane (20R); l = 24-ethyl-14 α (H),17 α (H)-cholestane (20R). All of these compounds are collectively referred to as steranes, and compounds a, b, g, and possible coeluting compounds in peaks c, d, e, and i are collectively referred to as diasteranes.

tively. The pH values in experiments 1, 3, and 5 (Table 7) increase from 5.8 to 7.2 as the amount of expelled oil increases with temperature (Table 2). This covariance suggests H^+ ions may be important to the generation of expelled oil. The importance of this ion is considered in experiment 16 by using a 0.1 N HCl solution in place of deionized water at 330°C for 70.7 h. As shown in Table 11, the final pH of this experiment increased to 4.7, but this final increased uptake and initial five-orders of magnitude increase in H^+ ions have no significant effect on the amounts of expelled oil and generated gas relative to experiments 10, 11, and 12. In addition, gas chromatograms of the expelled oils from

these experiments (Fig. 7) show no significant compositional differences.

In its molecular form, hydrogen has been shown to enhance oil yield and reduce aromatization and condensation during anhydrous pyrolysis of oil shale (Hershkowitz et al., 1983). Experiment 17 examines the role molecular hydrogen plays in hydrous pyrolysis by heating an aliquot of WD-26 at 330°C for 70.9 h with an initial 1.48 MPa of H_2 in the head-space of the reactor instead of the usual 241 kPa of He at the start of the experiment. Expelled oil and generated gas yields from this experiment (Table 11) are similar to the other hydrous experiments (10, 11, 12, and 16), with the

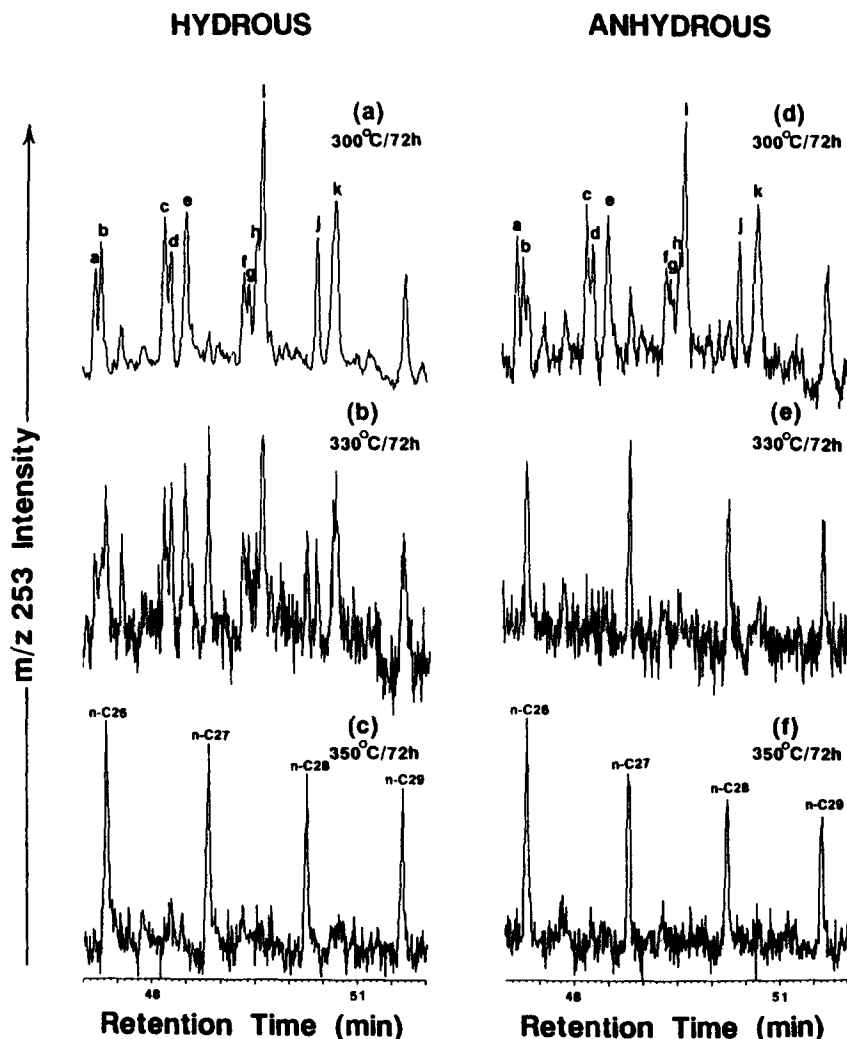


Fig. 6. m/z 253 ion chromatograms of the saturate fraction of the total pyrolysate from hydrous (a, b, and c) and anhydrous (d, e, and f) experiments. The peak designations are in reference to C-ring monoaromatic steroid hydrocarbons: a = $5\beta(\text{H})$ C_{27} (20S); b = DIA C_{27} (20S); c = $5\beta(\text{H})$ C_{27} (20R) plus DIA C_{27} (20R); d = $5\alpha(\text{H})$ C_{27} (20S); e = $5\beta(\text{H})$ C_{28} (20S) plus DIA C_{28} (20S); f = $5\alpha(\text{H})$ C_{27} (20R); g = $5\alpha(\text{H})$ C_{28} (20S); h = $5\beta(\text{H})$ C_{28} (20R) plus DIA C_{28} (20R); i = $5\beta(\text{H})$ C_{29} (20S) plus DIA C_{29} (20S); j = $5\alpha(\text{H})$ C_{29} (20S); k = $5\alpha(\text{H})$ C_{28} (20R); and l = $5\beta(\text{H})$ C_{29} (20R) plus DIA C_{29} (20R). Peaks designated with $n\text{-C}_{26}$ through $n\text{-C}_{29}$ represent normal alkanes with corresponding carbon numbers of 26 through 29.

exception of the additional molecular hydrogen. The slightly lower yields are most likely the result of the lower temperature attained in this experiment compared to those attained in experiments 10 and 11 (Table 1). Gas chromatograms of the expelled oils in Fig. 7 show no significant compositional variations between hydrous pyrolysis with and without the additional molecular hydrogen. These results indicate that the addition of H_2 does not influence the product yields under hydrous conditions as observed under anhydrous conditions.

The solubility of oil in water increases with increasing temperature (Price, 1976), but at 350°C the solubilities of the $\text{C}_{14}\text{--}\text{C}_{20}$, $\text{C}_{19}\text{--}\text{C}_{25}$, and $\text{C}_{24}\text{--}\text{C}_{34}$ distillation fractions of a 35.3° API gravity oil are only 0.85, 0.54, and 0.24 wt%, respectively (Price, 1981). Experiment 15 evaluates the influence of solubility by employing a 5.0 wt% NaCl solution. Substituting this saline solution for deionized water in the

experiment reduces the solubility of most hydrocarbons and oils by a factor of 2 (Whitehouse, 1984; Price, 1981; Sutton and Calder, 1974). The results in Table 11 show that the reduced oil solubility in experiment 15 enhances rather than reduces the expelled oil yield. At room temperatures under which the products are collected from the experiments, the solubility differences between deionized and saline waters may account in part for the slightly higher amounts of head-space gas, but they can not account for the significantly higher amount of expelled oil (Table 11). Comparisons of the gas chromatograms in Fig. 7 show that the expelled oil from experiment 15 has a composition similar to the other hydrous experiments (experiments 10, 16, and 17), with the exception of higher concentrations of C_5 through C_7 hydrocarbons. These results indicate that aqueous solubility of hydrocarbons is not responsible for the expelled oil gener-

Table 6. Concentration (mmol/400 g of rock) of gases collected in reactor headspace after hydrous and anhydrous experiments.

Condition Experiment no.	300°/72 h		330°C/72 h		350°C/72 h	
	hydrous 1	anhydrous 2	hydrous 3	anhydrous 4	hydrous 5	anhydrous 6
Methane	13.57	20.70	38.19	80.67	78.41	138.12
Ethane	8.19	13.75	25.63	49.78	43.57	1.54
Propane	3.44	6.12	9.34	18.43	16.17	25.88
<i>i</i> -butane	0.57	1.21	0.91	1.62	2.37	2.20
<i>n</i> -butane	1.53	1.90	2.83	6.07	4.52	10.71
Pentanes	0.48	0.82	1.39	2.10	0.79	1.95
Hexanes	0.00	0.21	0.00	0.00	0.00	0.00
C ₇ ^a	0.16	0.19	0.00	0.07	0.57	0.59
Ethene	0.02	0.00	0.00	0.00	0.14	0.10
Propene	0.45	0.23	0.00	0.00	0.41	0.56
Butenes						
Pentenes ^a	0.17	0.19	0.38	0.56	0.00	0.00
Hexenes ^a	0.00	0.01	0.00	0.00	0.00	0.00
Butadienes	0.01	0.03	0.07	0.00	0.03	0.03
CO ₂	20.07	14.39	31.17	20.88	44.01	21.56
CO	0.00	0.00	0.00	0.00	0.41	0.42
H ₂	5.06	5.38	5.89	8.25	6.07	11.86
H ₂ S	0.14	33.71	19.69	52.90	23.76	57.87
NH ₃	0.00	0.36	0.00	0.00	0.00	0.03
Total	53.96	99.20	135.49	241.38	222.94	346.00

^a Cyclic alkanes plus alkenes.

ated during hydrous pyrolysis. This finding is also supported by the results from experiment 12, which showed no significant increase in product yields with an increase in the water/rock ratio (Table 11).

3.4. Liquid Gallium-Alloy

Determining whether water in the hydrous experiments acts only as a liquid medium into which expelled oil is physically transferred requires an anhydrous experiment with a nonaqueous liquid. To ensure comparable results, the nonaqueous liquid should have a melting point below room temperature, a low solubility for hydrocarbons, a supercritical temperature above 330°C, and a specific gravity equal to or greater than one. Organic liquids like *n*-decane, isopropyl benzene, butyric acid, and heptanol maintain a subcritical liquid phase between 25 and 330°C, but have a high hydrocarbon solubilities. Conversely, inorganic liquids like stannic chloride, hydrogen fluoride, and sulfuric acid have relatively low hydrocarbon solubilities, but are not in the subcritical liquid phase over the temperature range of 25 to 330°C. Liquid metals like gallium and mercury offer the most promising comparison with water because of their liquid state within the desired temperature range and low hydrocarbon solubilities. In addition, gallium wets most surfaces including glass and has been reported to quickly diffuse into some metal crystal lattices (de la Breteque, 1978). Although its boiling point is 2200°C, the 30°C melting point results in a solid phase at typical room temperatures (i.e., 20 to 26°C). This problem is alleviated by using a gallium alloy containing 24.7 wt% indium (Indalloy 60, Indium Corporation of America), which has a melting point of 15.7°C. Results

from experiment 14 with the gallium alloy at 330°C for 70.6 h are compared in Table 12 with results from the average of hydrous experiments 10 and 11 and anhydrous experiment 4. No expelled oil was observed on the surface of the gallium-alloy liquid at the end of the experiment, but a floating, light-gray and reddish brown solid crust was observed and collected. This thin crust showed no signs of an oil or char film. X-ray diffraction identified the reddish-brown solid as In₂S₃ and the light-gray solid as a mixture of δ - and β -Ga₂O₃.

The amount of bitumen generated in this experiment is relatively high, but the lack of an expelled oil on the surface of the gallium-alloy liquid results in a total pyrolysate yield that is intermediate to those of the hydrous and anhydrous experiments. The amount of hydrocarbon gases generated in this experiment are similar to those generated in the anhydrous experiment (4, Table 12). However, amounts of nonhydrocarbon gases are significantly different. The most obvious difference is the 106 mmol of molecular hydrogen generated in the Ga-alloy experiment. It is this high partial pressure of H₂ that may account for the higher amount of bitumen relative to the anhydrous experiment and the intermediate amount of total pyrolysate. Although experiment 17 shows that molecular hydrogen under hydrous conditions has no significant effect on yields of total expelled products (Table 11), yields of condensable oil from retorting of oil shales are increased by the presence of molecular hydrogen under anhydrous conditions (Hershkowitz et al., 1983).

The anomalously large amount of molecular hydrogen generated in the Ga-alloy experiment is most likely the result of gallium oxidation by water. This reaction is sluggish at 100°C but rapid at 200°C (de la Breteque, 1978). The overall reaction involves water oxidizing gallium to a gallium

Table 7. Millimole of gas (g) and dissolved gas species (aq) generated from 400 g of Woodford Shale sample WD-26. Gas quantities are from Table 6 and dissolved species quantities are calculated as footnoted assuming ideal gas behavior at 25°C and an ionic strength of zero. Total gas quantities do not include species dissolved in expelled oil or bitumen. Dissolved species in minor amounts of water evolved during anhydrous pyrolysis are negligible relative to mmole units and are therefore not included in table.

Condition Experiment no.	300°C/72 h		330°C/72 h		350°C/72 h	
	hydrus 1	anhydrous 2	hydrus 3	anhydrous 4	hydrus 5	anhydrous 6
CO ₂ (g)	20.07	14.39	31.17	20.88	44.01	21.56
CO ₂ (aq) ^a	15.06	0.00	49.12	0.00	196.14	0.00
Total CO ₂	35.13	14.39	80.29	20.88	240.15	21.56
H ₂ S(g)	0.14	33.71	19.69	52.90	23.76	57.87
H ₂ S(aq) ^b	0.26	0.00	48.11	0.00	106.37	0.00
Total H ₂ S	0.40	33.71	67.80	52.90	130.13	57.87
H ₂ (g)	5.06	5.38	5.89	8.25	6.07	11.86
H ₂ (aq) ^c	0.07	0.00	0.08	0.00	0.08	0.00
pH	5.84	0.00	6.59 ^d	0.00	7.18	0.00
Total H ₂	5.15	5.38	5.97	8.25	6.15	11.86
CH ₄ (g)	13.57	20.70	38.19	80.67	78.41	138.12
CH ₄ (aq) ^c	0.15	0.00	0.92	0.00	1.89	0.00
Total CH ₄	13.72	20.70	39.11	80.67	80.30	138.12
C ₂ H ₆ (g)	8.19	13.75	25.63	49.78	43.57	71.54
C ₂ H ₆ (aq) ^c	0.26	0.00	0.82	0.00	1.40	0.00
Total C ₂ H ₆	8.45	13.75	26.45	49.78	44.97	71.54

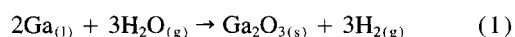
^a CO₂(aq) = H₂CO₃ + HCO₃⁻ + CO₃⁼ = K_HP_{CO₂} {1 + (K₁[H⁺]) + (K₁K₂/[H⁺]²)}, where P_{CO₂} = CO₂ gas partial pressure (atm), K_H = 10^{-1.470} mol/l-atm (Butler, 1982), [H⁺] = hydrous ion concentration (mol/l), K₁ = 10^{-6.352} for H₂CO₃ disassociation (Butler, 1982), and K₂ = 10^{-10.329} for HCO₃⁻ dissociation (Butler, 1982).

^b H₂S(aq) = H₂S⁰ + HS⁻ + S⁼ = K_HP_{H₂S} {1 + (K₁/[H⁺]) + (K₁K₂/[H⁺]²)}, where P_{H₂S} = H₂S gas partial pressure (atm), K_H = 10^{-0.99} mol/l atm (Carroll and Mather, 1989), [H⁺] = hydrogen ion concentration (mol/L), K₁ = 10^{-6.983} for H₂S disassociation (Hershey and others, 1988), and K₂ = 10^{-18.57} for HS⁻ dissociation (Schoonen and Barnes, 1988).

^c Moles of dissolved gas (m_i) determined by m_i = [m_{H₂O} (P_i/K_{H_i)]/[1 - (P_i/K_{H_i)], where P_i = partial pressure of gas i, m_{H₂O} = moles of H₂O (320 q/18 amu = 17.778 mol), and K_{H_i} = Henry's Law constant for gas i (70073.5 atm/mole fraction for i = H₂, Drummond, 1981; 39185.6 atm/mole fraction for i = CH₄, Rettrich et al., 1981; 29286.7 atm/mole fraction for i = C₂H₆, Rettich et al., 1981).}}

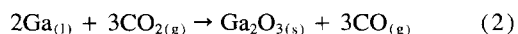
^d This is the mean pH of experiments 10 (6.61) and 11 (6.58), which were conducted under the same experimental conditions as experiment 3 (Table 1).

sesquioxide and the hydrogen in the water reducing to molecular hydrogen:



Water vapor in this experiment, as well as in the other anhydrous experiments (2, 4, 6, 7, and 8), is from pore and mineral waters in the original rock, and to a lesser extent, from dehydration of the kerogen. This water vapor condenses as liquid-water droplets on top of the inside of the reactor as it cools to room temperature. Semiquantitative collection of this intrinsic water typically accounts for about 1 wt% of the original rock after being heated at 300 and 330°C. This quantity of water is similar to that obtained from oil shales by Fischer assay (Coburn et al., 1989).

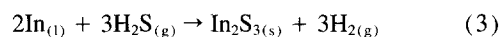
Another reaction responsible for the gallium sesquioxide is the interaction of CO₂ with the gallium:



Thermodynamics indicate this reaction is less favorable than reaction 1, but the generation of anomalous amounts of CO (Table 12) indicate this reaction may be a source of minor amounts of the gallium sesquioxide. Despite the loss of some

CO₂ by this reaction, the amount of CO₂ is intermediate to that of the hydrous and anhydrous experiments (Table 12).

Although In₂O₃ has a crystal structure analogous to metastable δ-Ga₂O₃, no significant solid solution between these oxides occurs (Roy et al., 1952). Thermodynamic data indicate that Ga has a greater affinity for oxide formation than In (Srivastava and Farber, 1978), and that In has a greater affinity for sulfide formation than Ga (Mukdeeprom and Edwards, 1987). These different affinities explain the absence of In-oxides and the presence of In-sulfide in the floating solid crust. The preferred interaction of In with H₂S is



which results in the generation of molecular hydrogen and In₂S₃. As a result of this reaction, the amount of H₂S recovered from this experiment is reduced relative to the anhydrous experiment (4, Table 12).

3.5. D₂O-Experiment

Hoering (1984) conducted experiments using D₂O and pre-extracted Messel Shale with and without molecular probes to gain insight on the role of water in hydrous pyroly-

Table 8. Mass balance of sulfur and oxygen lost from pyrolyzed kerogen relative to the amount of H₂S and CO₂ generated under hydrous and anhydrous conditions.

Temp./time	300°C/72 h		330°C/72 h		350°C/72 h	
	Condition	Condition	Condition	Condition	Condition	Condition
Experiment no.	1	2	3	4	5	6
Kerogen S remaining ^a (mmol)	208.60	199.33	156.09	157.56	129.81	135.10
Kerogen S lost ^b (mmol)	20.32	29.59	72.83	71.36	99.11	93.82
S as Total H ₂ S ^c (mmol)	0.40	33.71	67.80	52.90	130.13	57.87
ΔS ^d (mmol)	+19.92	-4.12	+5.03	+18.46	-31.02	+35.95
Kerogen O remaining ^e (mmol)	590.45	544.56	414.40	440.12	382.98	441.76
Kerogen O lost ^f (mmol)	99.23	145.12	275.28	249.56	306.69	247.92
O as Total CO ₂ ^g (mmol)	70.26	14.39	160.58	41.76	480.30	43.12
ΔO ^d (mmol)	+28.97	+116.34	+114.70	+207.80	-173.61	+204.80

^a Milimoles of kerogen sulfur in recovered rock = $31.19 \{S_K/C_K[C_E/(100 - B)]\} \{W_i - E - G\}$, where S_K and C_K are, respectively, the weight percent organic sulfur and carbon of isolated kerogen (Table 4), C_E is weight percent of kerogen carbon of solvent-extracted rock (Table 4), B is weight percent of bitumen in recovered rock (Table 2), E and G are, respectively, wt% of expelled oil and gas from original rock (Table 2), W_i = grams of original rock (Table 1), and 31.19 is the reciprocal of the atomic mass of S multiplied by 10³.

^b Difference between organic S in kerogen of the original 400 grams of rock (i.e., 228.92 mmol) and kerogen S remaining in recovered rock.

^c Values include gas and dissolved gas species from Table 7.

^d f notation refers to differences between kerogen S or O lost and S or O as total H₂S or CO₂, respectively.

^e Millimoles of kerogen oxygen in recovered rock = $62.5 \{O_K/C_K[C_E/(100 - B)]\} \{W_i - E - G\}$, where C_K , C_E , B , W_i , E , and G are the same as defined in footnote a, and O_K is the weight percent oxygen of isolated kerogen (Table 4). The coefficient 62.5 is the reciprocal of the atomic mass of O multiplied by 10³.

^f Difference between O in kerogen of the original 400 grams of rock (i.e., 689.68 mmol) and kerogen O remaining in recovered rock.

sis experiments. Results from these experiments demonstrate that deuterium substitution with hydrogen in the hydrocarbon products is not a simple homogeneous exchange reaction, but instead involves deuteration of hydrocarbon radicals cleaved from the pyrolyzed kerogen. Hoering (1984) suggested exchange of hydrogen radicals with D₂O to yield deuterium radicals, which deuterate and terminate hydrocarbon radicals. The shale sample used in his experiments was ground in a ball-mill and the organic matter in the resulting rock powder would be well exposed to the D₂O. Petrographic studies of rock chips and cores subjected to hydrous pyrolysis indicate rock matrices become impregnated with bitumen and devoid of interstitial water during the early stages of bitumen generation (Lewan, 1993a, 1987). This bitumen saturation limits the contact between water and organic matter to the outer surface of the rock chips or core. Experiment 13 was conducted to determine the degree of deuteration of

organic matter embedded in the gravel-sized (0.5 to 2.0 cm) rock chips of sample WD-26. As shown in Table 13, amounts and types of product from this experiment are similar to those from the H₂O experiments conducted at similar time and temperature conditions (10 and 11).

The amounts of deuterium in the expelled oil, extracted bitumen, and isolated kerogen from experiment 13 with D₂O and experiment 11 with H₂O were determined by deuterium-NMR analyses (Spectral Data Services, Inc.). None of the pyrolysate products from the H₂O experiment (experiment 11) contained detectable amounts of deuterium. Conversely, all of the pyrolysate products from the D₂O experiment (experiment 13) contained detectable amounts of deuterium. Quantification of deuterium content of the kerogen was not performed, but the NMR spectrum of the kerogen isolated from the recovered rocks in experiments 11 and 13 (Fig. 8) show that the kerogen in the D₂O experiment was highly

Table 9. Types and amounts (wt% of rock) of pyrolysates generated in hydrous, anhydrous, and confined pressure experiments on Woodford Shale sample WD-26 at 350°C for 72 h.

Conditions	Hydrous	Vacuum anhydrous	He-pressured anhydrous	Confined-gas anhydrous	Steam pyrolysis
Final pressure ^a (MPa)	21.13	5.69	23.48	21.76	18.31
Experiment no.	5	6	7	8	9
Bitumen extract	5.71	3.30	2.99	2.27	6.01
Expelled oil	4.15	0.00	0.00	0.00	0.00
Generated gas	1.68	2.40	2.18	2.57	2.08
Total pyrolysate	11.54	5.70	5.17	4.84	8.09

^a Pressure in reactor at 350°C after 72 h.

Table 10. Concentration (mmol/400 g rock) of gases collected from reactor headspace after hydrous, anhydrous, and steam experiments cooled to room temperature.

Conditions	Hydrous	Vacuum anhydrous	He-pressured anhydrous	Confined-gas ^b anhydrous	Steam pyrolysis
Final pressure at 350°C (MPa)	21.13	5.69	23.48	21.76	18.31
Experiment	5	6	7	8	9
Methane	78.41	138.12	114.76	206.26	88.14
Ethane	43.57	71.54	59.67	72.07	53.33
Propane	16.17	25.88	23.69	23.73	19.17
<i>i</i> -butane	2.37	2.20	7.42	2.34	2.26
<i>n</i> -butane	4.52	10.71	7.71	5.16	7.67
Pentanes	0.79	1.95	0.00	2.02	0.86
Hexanes	0.00	0.00	0.00	0.00	0.00
C ₇ +	0.57	0.59	4.85	0.00	0.79
Ethene	0.14	0.10	3.99	0.12	0.17
Propene	1.71	2.58	11.70	0.00	2.77
Butenes	0.41	0.56	0.00	0.00	0.45
Pentenes ^a	0.00	0.00	0.00	0.44	0.00
Hexenes ^a	0.00	0.00	0.00	0.00	0.00
Butadienes	0.03	0.03	0.00	0.00	0.00
CO ₂	44.01	21.56	23.12	42.98	51.97
CO	0.41	0.42	1.14	0.00	0.55
H ₂	6.07	11.86	15.13	1.59	8.66
H ₂ S	23.76	57.87	29.40	37.46	38.44
NH ₃	0.00	0.03	1.43	0.00	0.10
Total	222.94	346.00	304.01	394.17	274.33

^a Cyclic alkanes plus alkenes.

^b Recalculated on the basis of 400 g of rock.

deuterated. An internal standard of deuterated dichloromethane was used to quantitatively determine deuterium contents of 10.3 wt% for the expelled oil and 6.6 wt% for the extracted bitumen. Calculating the total weight percentages of deuterium on a molar basis with the yields in Table 13 gives 141 and 312 mmol of deuterium for the expelled oil and extracted bitumen, respectively. Assuming the hydrogen contents of the expelled oil are similar to the 13 wt% average for crude oil (Hunt, 1979) and that the extracted bitumen is similar to the 10 wt% average for asphalt (Hunt, 1979), deuterium substitution for hydrogen is approximately 40% for the expelled oil and 33% for the extracted bitumen. These percentages are only approximations, but they indicate deuteration is not limited to the outer surface of the rock chips, and some form of deuterium (e.g., D⁺, D₂, HDO, and D₂O) penetrates the rock through its bitumen network. The implication here is that while the movement of oil and bitumen is outward from within the rock, the movement of some form of deuterium is inward into the bitumen impregnated rock from the surrounding D₂O liquid. Generated hydrocarbon gases including methane were also deuterated, but no attempt was made to quantify their degree of deuteration. Although the separation of D₂ from He was marginal for quantification by mass spectrometry, an analysis of the generated gas gave a D₂ content of 1 mol%.

3.6. Isolated Kerogen Experiment

Some minerals within source rocks have been advocated as catalysts in petroleum formation (Brooks, 1952; Goldstein, 1983). Tannenbaum et al. (1986) conducted hydrous

pyrolysis experiments on artificial mixtures of minerals and isolated kerogens in borosilicate glass tubes at 300°C for durations from 2 to 1000 h. Pyrolysate yields from these hydrous experiments were essentially the same for kerogens heated with and without minerals. As discussed by Lewan (1993a), the use of borosilicate glass tubes, the inability to collect expelled oil, and the unconsolidated state of the powdered mixtures makes these experiments difficult to compare with whole-rock hydrous experiments, which are more representative of natural petroleum formation. In order to make a more appropriate evaluation of the effects mineral matter has on the role of water in petroleum formation, experiment 18 was conducted with a kerogen isolated from sample WD-26. As described in section 2, precautions were taken to insure that a water-wet kerogen resided at the bottom of the reactor during the experiment. The experiment was conducted at 330°C for 72 h under hydrous conditions. An expelled oil similar to that generated from whole-rock experiments was present on the water surface at the conclusion of this experiment. After the generated gas, expelled oil, and water were collected, a glossy black, vesicular solid was removed from the bottom of the reactor. This solid was brittle, which allowed it to be broken up for Soxhlet extraction to determine its bitumen content. The amounts of pyrolysates generated in this experiment are given in Table 13 on the basis of an equivalent rock weight to facilitate comparisons with the other experiments in this study. Relative to the whole-rock experiments (10 and 11), the amounts of bitumen, expelled oil, and gas generated in the kerogen experiment are slightly greater (Table 13). The slightly greater amounts of bitumen and expelled oil in the kerogen

Table 11. Experimental conditions and expelled product (expelled oil and gas) yields of hydrous pyrolysis experiments with various water chemistries.

Condition Experiment	Water/rock ratio 0.8 10	Water/rock ratio 0.8 11	Water/rock ratio 2.25 12	0.1 N HCl hydrous 16	H ₂ -pressured hydrous 17	5 wt% NaCl hydrous 15
Temperature (°C)	330.0	329.7	329.9	329.5	327.6	329.79
Duration at temperature (h)	70.70	70.70	70.85	70.70	70.70	70.55
Initial pH	5.65 ^a	5.65 ^a	5.65 ^a	1.00	5.65 ^a	5.65 ^a
Final pH	6.61	6.58	6.21	4.68	6.70	6.00
Expelled oil (wt% rock)	2.66	2.69	2.75	2.61	2.53	3.80
Gas (wt% rock)	1.55	1.40	1.29	1.36	1.27	1.53
Total expelled product (wt% rock)	4.21	4.09	4.04	3.97	3.80	5.33
Gas composition (mmol/400 g rock)						
Methane	49.34	48.51	36.24	45.87	39.97	52.38
Ethane	32.62	30.91	25.27	30.63	29.79	34.36
Propane	12.23	11.74	10.20	11.40	10.17	12.46
<i>i</i> -butane	1.85	1.77	1.89	1.43	1.03	0.90
<i>n</i> -butane	3.44	3.39	3.97	3.79	3.51	4.30
Pentanes	1.12	1.14	1.68	1.76	1.62	1.88
C ₆ +	0.00	0.14	0.37	0.07	0.00	0.00
Ethene	0.00	0.58	0.05	0.00	0.00	0.00
Propene	0.00	0.00	0.32	0.00	0.02	0.00
Butenes	0.00	0.00	0.03	0.00	0.00	0.00
Pentenes ^b	0.55	0.35	0.53	0.37	0.37	0.62
Hexenes ^b	0.00	0.00	0.35	0.16	0.27	0.00
Butadienes	0.00	0.07	0.05	0.07	0.08	0.00
CO ₂	48.67	40.86	39.68	39.74	32.75	44.66
CO	0.97	0.00	0.00	0.61	0.58	0.00
H ₂	4.32	6.25	11.32	6.53	49.93	7.94
H ₂ S	37.78	32.56	29.61	30.10	34.36	36.48
NH ₃	0.50	0.00	0.64	0.45	0.65	0.18

^a Values assume deionized (ASTM Type-1) water is in equilibrium with atmospheric CO₂ according to calculations by Butler (1982).

^b Alkenes plus cyclic alkanes.

experiment may be attributed to the lack of adsorptive mineral surfaces, which have been shown to reduce the amounts of extractable bitumen (Spiro, 1984; Huizinga et al., 1987) and volatile hydrocarbons (Espitalie et al., 1980; Horsfield and Douglas, 1980) from pyrolyzed mineral-kerogen mixtures. The slightly greater amount of generated gas in the kerogen experiment is a result of all the gas components increasing to different degrees, with the exception of the decrease in methane (Table 14). As observed in other comparisons between gas generated from rocks and their isolated kerogens (Lewan, 1993a), alkene gas concentrations are higher in the isolated kerogen experiment. Based on these results, the role of water in generating bitumen and expelled oil is slightly influenced by the presence of a mineral matrix. However, the presence of a mineral matrix has a more notable influence on the composition and quantities of generated gas.

4. DISCUSSION

Hydrous pyrolysis experiments at temperatures between 240 and 365°C for 72 h on aliquots of Woodford Shale (Lewan, 1983), Phosphoria Shale (Lewan et al., 1986), Monterey Shale (Baskin and Peters, 1992), and Green River Shale (Huizinga et al., 1988; Ruble, 1996) show that petroleum formation can be described by two overall reactions that generate distinctly different products. The first reaction involves the partial decomposition of the kerogen to bitumen

at temperatures equal to or less than 330°C after 72 h. As the bitumen content increases during this overall reaction, the initial kerogen content decreases proportionally. There is a net volume increase resulting from this reaction which causes the generated bitumen to impregnate the available porosity in the rock and form a continuous bitumen network throughout the rock matrix (Lewan, 1987). The generated bitumen remains in the rock matrix and consists of a viscous tar enriched in high-molecular-weight polar components and deficient in saturated hydrocarbons. The second reaction involves the partial decomposition of the bitumen to oil at higher thermal stress levels (e.g., $\geq 330^\circ\text{C}$ after 72 h). As the amount of expelled oil increases during this overall reaction, the bitumen content decreases proportionally and the kerogen content remains essentially constant. The net volume increase caused by this reaction, and the lack of porosity due to the impregnating bitumen, results in the expulsion of generated oil from the rock. This expelled oil accumulates on the water surface and typically consists of a free-flowing liquid enriched in saturated hydrocarbons and deficient in high-molecular-weight polars. These two overall reactions have long been recognized in oil shale retorting (Engler, 1913; Hershkowitz et al., 1983) and have been suggested in natural petroleum formation (Louis and Tissot, 1967). Distinguishing and understanding these two overall reactions is an important prerequisite to evaluating the role of water. The yields given in Table 2 and previously reported hydrous-pyrolysis yields on the Woodford Shale (Lewan, 1983) indi-

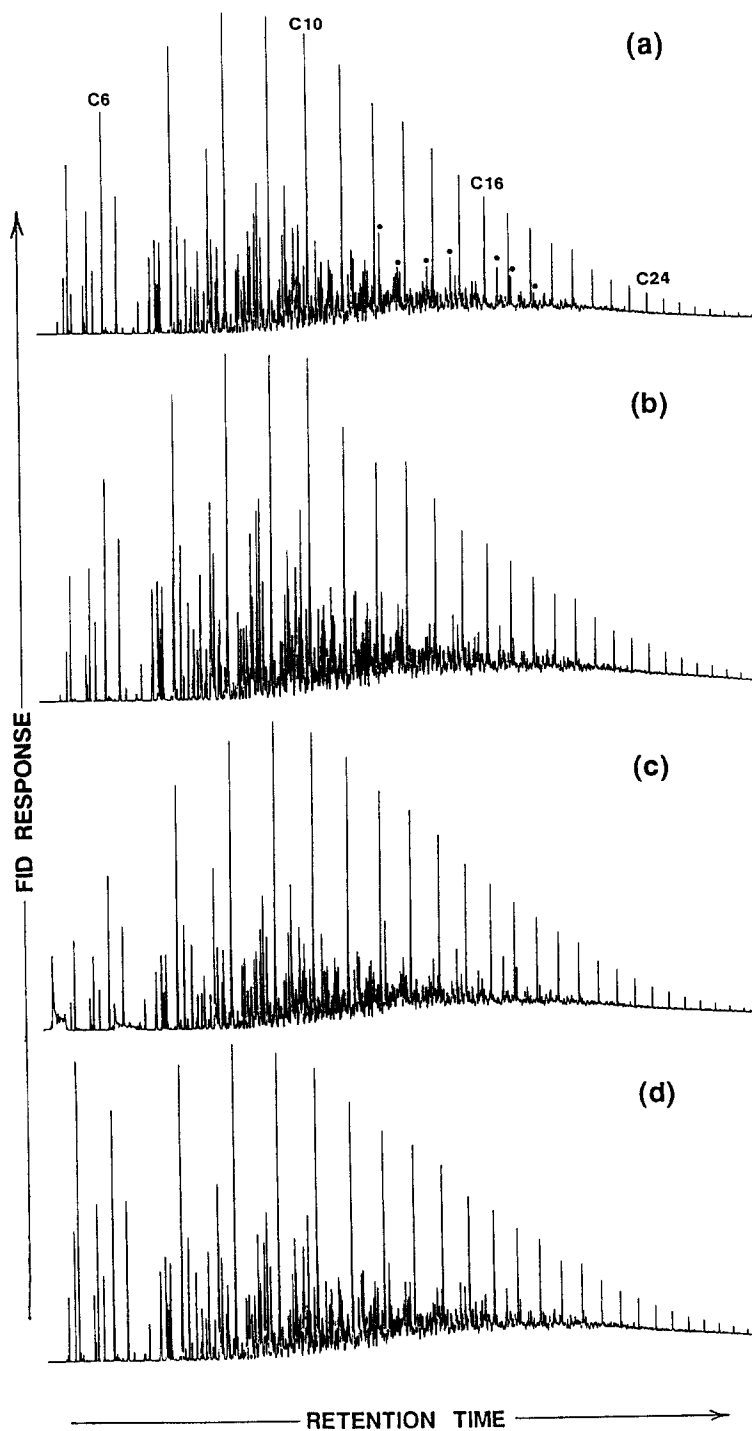


Fig. 7. Gas chromatograms of expelled oils from (a) hydrous experiment 10; (b) 0.1 N HCl experiment 16; (c) H₂-pressured experiment 17, and (d) 5 wt% NaCl hydrous experiment 15. Prominent peaks represent *n*-alkenes with carbon numbers denoted for *n*-hexane (C₆), *n*-decane (C₁₀), *n*-hexadecane (C₁₆), and tetracosane (C₂₄). Solid dots (●) denote acyclic isoprenoids with 13 through 16 and 18 through 20 carbon atoms.

cate that experiment 1 at 300°C for 72 h represents the first overall reaction (i.e., kerogen to bitumen) and experiments 3 and 5 at 330°C and 350°C for 72 h represent the second overall reaction (i.e., bitumen to oil). The following discussion evaluates the role of water in different phases, bitumen generation, oil generation, hydrogen generation, and oil separation from bitumen.

4.1. Water Phases

Before discussing the specific role of water in petroleum formation, it is important to evaluate the water phases that occur within the experiments. The two most obvious water phases that occur within the hydrous pyrolysis experiments are liquid and vapor water. As described by Lewan (1993a),

Table 12. Product yields and gas analyses of the gallium-indium (Ga/In) experiment 14 compared to vacuum anhydrous experiment 4 and the average of hydrous experiments 10 and 11.

Conditions Experiment no.	Hydrous 10 ± 11	Anhydrous 4	Ga/In 14
Product yields (wt% of Rock)			
Bitumen	7.85	6.62	8.12
Expelled	2.68	0.00	0.00
Gas	1.48	1.74	1.88
Total pyrolysate	12.01	8.36	10.00
Gas analyses (mmol/400 g rock)			
Methane	48.93	80.67	80.86
Ethane	31.77	49.78	53.40
Propane	11.99	18.43	19.79
<i>i</i> -butane	1.81	1.62	2.52
<i>n</i> -butane	3.42	6.07	5.40
Pentanes	1.13	2.10	1.77
Hexanes	0.07	0.00	0.00
C ₇ +	0.00	0.07	0.00
Ethene	0.29	0.00	0.00
Propene	0.00	0.05	0.00
Butenes	0.00	0.00	0.00
Pentenes ^a	0.45	0.56	0.91
Butadienes	0.03	0.00	0.00
CO ₂	44.77	20.88	37.86
CO	0.49	0.00	2.52
H ₂	5.29	8.25	105.94
H ₂ S	35.17	52.90	33.62
NH ₃	0.25	0.00	0.25
Total	185.86	241.38	344.84

^a Cyclic alkanes plus alkenes.

the amount of rock and water added to a reactor are predetermined to ensure that the rock remains submerged in liquid water at ambient and experimental temperatures. Water vapor is restricted to the gas head-space above the liquid-water surface, which constitutes approximately 30 to 15 vol% of the reactor volume at typical experimental temperatures. Supercritical water is avoided in the experiments by employing experimental temperatures less than 374°C (i.e., critical temperature for pure water) or by employing NaCl solutions, which can elevate the supercritical temperature of water (Sourirajan and Kennedy, 1962; Haas, 1976).

Another important aspect of these experiments that must be considered in discussing the role of water is that the reactions responsible for petroleum formation occur within the bitumen-impregnated, gravel-sized rock chips and not within the water surrounding the rock chips. Although ancillary reactions involving the surrounding water with mineral, bitumen, or kerogen exposed on the outer surfaces of the rock chips may occur, the principal reactions are occurring within the bitumen-impregnated rock, as is the condition in natural systems. The external water surrounding the rock chips in the experiments may be considered analogous to the water in regional fractures that commonly dissect source rocks in the natural system. The subordinate role of the external water is demonstrated by the lack of change in types and amounts of yield when the water to rock ratio is approximately tripled in experiment 12, and when the area of exposed rock surface is increased by using a smaller sized rock chip in the experiments (Lewan, 1993a). Realizing that the bulk liquid water phase in these experiments is external to reaction sites within the heated rock becomes important when comparing the results of this study with experiments that use finely-ground rock powders (e.g., Hoering, 1984), unconsolidated mixtures of mineral and kerogen powders (e.g., Tannenbaum et al., 1986), and model compounds (e.g., Siskin et al., 1990). In these experiments, the contact of reacting organic matter with a bulk liquid water phase is maximized and not representative of the natural system. Model compound studies present an additional complication in that the studied compounds may react as aqueous species dissolved in the liquid water. Although this condition may represent localized conditions during secondary migration or entrapment of petroleum in the natural system, it is not likely to represent the conditions under which petroleum is generated in bitumen-impregnated source rocks.

Prior to the generation of bitumen, the porosity of the heated rock contains liquid water that may or may not be in communication with the external water surrounding the rock, depending on the permeability of the rock. This porewater will remain liquid water during hydrous pyrolysis but will become undersaturated water vapor during anhydrous pyrolysis. The latter condition results in condensation of the water vapor to liquid water droplets that occur on rock and reactor-wall surfaces after anhydrous experiments have cooled to

Table 13. Type and amounts (wt%) of pyrolysates generated at 300°C from WD-26 rock and isolated kerogen under hydrous conditions with D₂O or H₂O.

Condition Experiment	D ₂ O-Rock 13		H ₂ O-Rock 10 + 11		H ₂ O-Kerogen ^b 18	
	Rock basis	Pyrolysate basis	Rock basis	Pyrolysate basis	Rock basis	Pyrolysate basis
Wt%						
Bitumen ^a	9.44	69.3	9.11	68.7	9.18	67.1
Expelled oil	2.73	20.0	2.68	20.2	2.74	20.0
Gas	1.46	10.7	1.48	11.1	1.76	12.9
Total pyrolysate	13.63	100.0	13.27	100.0	13.68	100.0

^a Bitumen is extracted in a Soxtec apparatus with dichloromethane, rather than in a Soxhlet apparatus with benzene/methanol, which was used to derive the bitumen values in Tables 2, 9, and 12.

^b Yields are calculated as wt% of rock based on the isolated kerogen comprising 29.56 wt% of the rock.

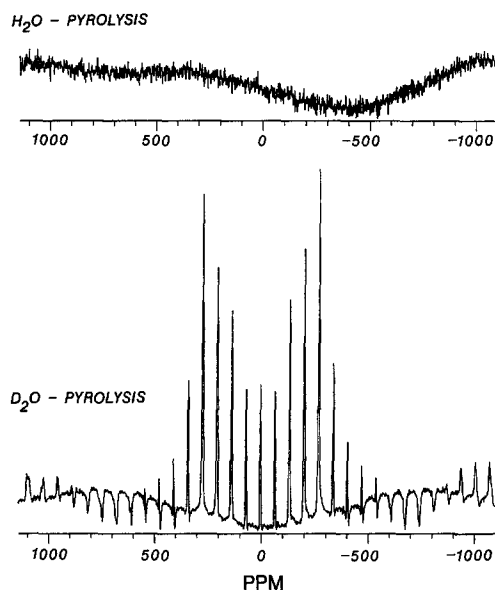


Fig. 8. D-NMR spectra of kerogen isolated from recovered rocks from hydrous pyrolysis experiments conducted at 330°C for 72 h with H₂O (experiment 11) and D₂O (experiment 13).

room temperatures. These condensed water droplets were observed in all the anhydrous pyrolysis experiments, including the one employing liquid metal (experiment 14). Porosities of thermally immature shales vary from 5 to 20 vol% (Rieke and Chilingarian, 1974), which equates to approximately 2 to 10 wt% pore water, assuming a grain density of

Table 14. Concentration (mmol/400 g rock) of gases collected from reactor headspace after heating at 330°C for 72 h.

Conditions Experiment no.	H ₂ O-rock ^a 10 + 11	H ₂ O-kerogen ^b 18
Gas components (mmol/400 g rock)		
Methane	48.93	44.09
Ethane	31.77	33.30
Propane	11.99	18.03
<i>i</i> -butane	1.81	2.82
<i>n</i> -butane	3.42	5.92
Pentanes	1.13	2.17
Hexanes	0.07	0.68
C ₇ +	0.00	0.65
Ethene	0.29	0.48
Propene	0.00	4.51
Butenes	0.00	0.00
Pentenes ^c	0.45	0.51
Butadienes	0.03	0.00
CO ₂	44.77	48.40
CO	0.49	0.45
H ₂	5.29	8.70
H ₂ S	35.17	39.07
NH ₃	0.25	1.16
Total	185.86	210.92

^a Mean of experiments 10 and 11.

^b Calculated on the basis of 29.56 wt% of the rock containing kerogen.

^c Cyclic alkanes plus alkenes.

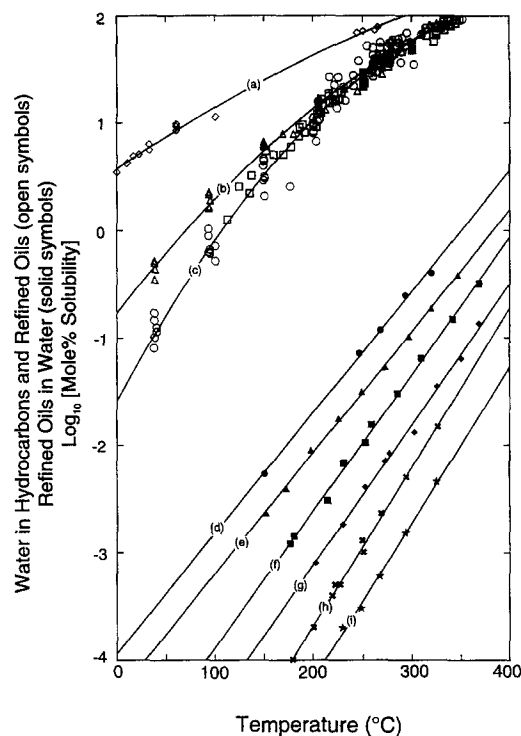


Fig. 9. Solubility (mol%) of water in glyceride-rich plant oils [open diamonds described by 2-degree polynomial curve (a), Hilder, 1968, 1971]; aromatic hydrocarbons [open triangles described by 2-degree polynomial curve (b), Guerrant, 1964; Brady et al., 1982; Tsionopoulos and Wilson, 1983]; aliphatic hydrocarbons [open circles described by 2-degree polynomial curve (c), Guerrant, 1964; Brady et al., 1982; Tsionopoulos and Wilson, 1983; Skripka and Boksha, 1976]; refined oil fractions including gasoline, kerosene, diesel, heavy diesel, and lubricating oil [open squares; Guerrant, 1964; Skripka, 1976; Griswold and Kasch, 1942], and solubility (mol%) of refined crude oil distillation fractions designated as C₁-C₁₀ [solid circles described by linear curve (d)]; C₆-C₁₀ [solid triangles described by linear curve (e)]; C₁₀-C₁₅ [solid squares described by linear curve (f)]; C₁₄-C₂₀ [solid diamonds described by linear curve (g)]; C₁₉-C₂₅ [solid crosses described by linear curve (h)]; and C₂₄-C₃₄ [solid stars described by linear curve (i)] in water (Price, 1981).

2.3 g/cm³. As bitumen expands into the rock matrix with increasing thermal maturity, the porewater is displaced by and dissolved in the impregnating bitumen. The amount of water displaced and dissolved depends on the proportionality of generated bitumen to porewater, the type of organic matter, and the experimental conditions. The low solubility of hydrocarbons in liquid water (Price, 1981) intuitively suggests that displacement is the dominant process. However, the solubility of water in hydrocarbons is two orders of magnitude higher than the solubility of hydrocarbons in water (Griswold and Kasch, 1942; Guerrant, 1964; Brady et al., 1982). As shown in Fig. 9, the solubility of water in various types of organic liquids increases exponentially with increasing temperature. Aromatic hydrocarbons can solubilize more water than aliphatic hydrocarbons, and organic liquids rich in heteroatom functional groups (e.g., glyceride-rich plant oils) can solubilize more water than aromatic hydrocarbons. At 250°C, aliphatic hydrocarbons can solubilize 30 mol% water, and glyceride-rich oils can solubilize 65

mol% water (Fig. 9). These mole percentages indicate that for every ten methylene units (i.e., $-\text{CH}_2-$) in a bitumen molecule there are 3.3 to 14.4 dissolved water molecules at 250°C. Therefore, a significant amount of water may be available in the bitumen network of a maturing source rock during hydrous pyrolysis. This dissolved phase is especially important in providing a means by which D_2O can penetrate a bitumen-impregnated rock and extensively deuterate the bitumen and kerogen within a rock as observed in experiment 13. The external water acts only as a source of dissolved water that maintains a water-saturated bitumen within a rock, and as an accommodating media in which generated oil may be expelled.

4.2. Bitumen Generation

The formation of bitumen as an intermediate to kerogen decomposition and oil generation involves the breaking of weak bonds within the kerogen, rather than mineral catalysis. Mineral catalysis is not likely because the same amount of bitumen is generated from isolated kerogen as from kerogen within the mineral matrix of a rock subjected to hydrous pyrolysis at 330°C for 72 h (Table 13, experiments 10, 11, and 18). The nature of weak bonds in kerogens has not been resolved, but low activation energies less than 20 kcal/mol have been determined on extractable bitumen from naturally matured source rocks ($E_a = 11.7$ to 20.0 kcal/mol; Tissot, 1969; Connan, 1974), extractable bitumen from hydrous pyrolysis experiments ($E_a = 17.1$ kcal/mol; Barth et al., 1989), and nonvolatile soluble bitumen from oil shale retorting ($E_a = 10.7$ to 19.0 kcal/mol; Braun and Rothman, 1975; Cummins and Robinson, 1972). These low activation energies are not representative of covalent-bond cleavage (i.e., >50 kcal/mol; March, 1985), and suggest that weak noncovalent bonds (e.g., multiple hydrogen bonds and electron donor/acceptor complexes) may be responsible. Weak noncovalent bonds have been proposed to explain the retention of bitumen as an insoluble component in coal structures at low thermal maturities (Kirchko and Gagarin, 1990). In addition, reductions in the molecular weights of well-characterized hydrocarbon polymers during the early stages of their thermal decomposition have been attributed to weak noncovalent bonds (Madorsky, 1964; Malhotra et al., 1975). Chiantore et al. (1985) report an activation energy of 7 kcal/mol for the several-fold reduction in molecular weight of polystyrene during the early stages of its thermal decomposition.

Although low activation energies of this magnitude can not be reasonably extrapolated to natural conditions in sedimentary basins (e.g., Lewan and Fisher, 1994), they indicate that kerogen decomposition to bitumen occurs at lower thermal stress levels than bitumen decomposition to oil, which typically has activation energies more representative of covalent bond cleavage. Despite these uncertainties in bond types and mechanisms responsible for bitumen generation, water does not appear to have a significant role on the overall amount of bitumen generated, as shown by the similar bitumen yields generated under hydrous and anhydrous conditions at 300°C after 72 h (Table 2, experiments 1 and 2). However, the measured biomarker parameters (Table 5)

show that the anhydrous condition promotes molecular changes within the bitumen that reflect higher thermal maturities. Similarly, a higher amount of generated gas (Table 2), lower Rock-Eval S_2 peak (Table 3), lower kerogen atomic H/C ratio, and higher kerogen NMR aromaticity (Table 4) produced under the anhydrous condition at 300°C after 72 h (experiment 2) indicate that maturation within the residual kerogen is enhanced in the absence of water.

4.3. Oil Generation

Kinetic studies on the partial decomposition of bitumen to oil give activation energies that range from 34 to 69 kcal/mol (Lewan, 1985, 1989; Lewan and Buchardt, 1989; Huizinga et al., 1988; Ruble, 1996). These values are similar to those determined for the thermal cracking of hydrocarbon and acrylate polymers (Madorsky and Straus, 1954; Madorsky, 1953), and indicate that cleavage of covalent bonds are responsible for the overall reaction of bitumen to oil. It is in this overall reaction that water plays its most obvious role and distinguishes hydrous pyrolysis from anhydrous pyrolysis. At 330 and 350°C after 72 h, the total pyrolysate yields (i.e., bitumen + oil + gas) from the WD-26 sample by hydrous pyrolysis are, respectively, 1.4 and 2.0 times greater than by anhydrous pyrolysis (Table 2, experiments 3–6). Similar differences in total pyrolysate yields from oil-prone kerogens have also been observed in other studies comparing hydrous and anhydrous pyrolysis, with total pyrolysate yields from hydrous pyrolysis being 1.7 and 1.8 times greater than total pyrolysate yields from anhydrous pyrolysis (Comet et al., 1986; Tannenbaum et al., 1986). Results from anhydrous and hydrous pyrolysis experiments at 330 and 350°C for 72 h show that these differences are reflected not only in the lack of an expelled oil in anhydrous pyrolysis but also in a reduced extractable bitumen (Table 2). More gas is generated by anhydrous pyrolysis, but the increased amount is insufficient to make up for the reduced bitumen and oil yields (Table 2).

This total-pyrolysate deficit from anhydrous pyrolysis indicates that a portion of the potential product capable of being generated under hydrous conditions as an expelled oil is instead becoming an insoluble product under anhydrous conditions. Cross-linking reactions, in which covalent bonds develop between adjacent inter- or intra-molecular carbons, are the most likely cause of this reduced yield. Conversely, cracking reactions, in which carbon-carbon bonds are broken, are the cause of enhanced yields due to oil generation under hydrous conditions. Both of these reaction pathways compete under the same thermal stress conditions, with the thermal-cracking pathway resulting in lower-molecular-weight soluble products (i.e., expelled oil) and the cross-linking pathway resulting in higher-molecular-weight insoluble products (i.e., pyrobitumen or char). Understanding these two competing reaction pathways has been critical to optimizing product yields in coal liquefaction (Bockrath et al., 1987) and oil-shale retorting (Stout et al., 1976). Open-system pyrolysis of oil-shales and coals promotes the cracking pathway at the expense of the cross-linking pathway by heating samples rapidly to high temperatures under low pressures and removing vaporized products quickly from the

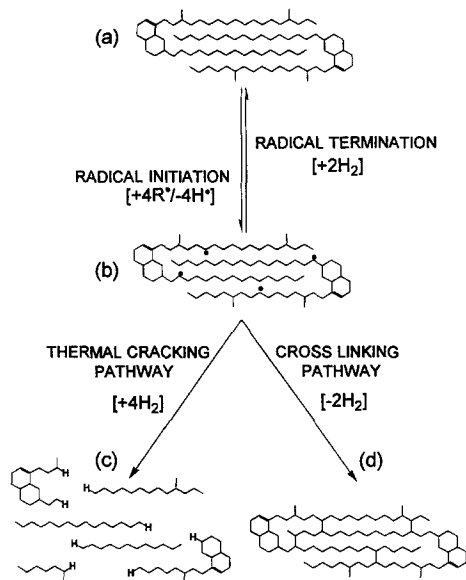


Fig. 10. Generalized reaction scheme for pyrolysis of a hypothetical bitumen molecule (a). As extraneous free radicals ($R\cdot$) abstract hydrogen ($H\cdot$) from the molecule, a transition-state molecule (b) with free-radical sites develops. The transition-state molecule may react with available molecular hydrogen to form the original bitumen molecule (a), undergo thermal cracking at the β -positions of the free-radical sites to form lower-molecular-weight hydrocarbon molecules (c), or undergo cross linking between radical sites and adjacent carbons to form a more cyclic and insoluble molecule (d).

heated sample to lower-temperature collection sites (Campbell et al., 1978; Solomon et al., 1990). Closed-system pyrolysis, as used in this study, can promote the cracking pathway at the expense of the cross-linking pathway by increasing the amount of molecular hydrogen within a reactor (Hershkowitz et al., 1983).

The wide distribution of molecular-weight n -alkanes (i.e., C_5 – C_{37}) and the low concentration of branched alkanes in the products generated by hydrous and anhydrous pyrolysis (Fig. 7) are indicative of a free-radical mechanism (Greensfelder and Voge, 1945; Beltrame et al., 1989). The two reaction pathways may be simply described by a free-radical mechanism as shown in Fig. 10. The initiation step in both reaction pathways is the formation of free-radical sites on a bitumen molecule by abstraction of hydrogen atoms through encounters with free radicals (e.g., $R\cdot = H_3C_2\cdot, H_3C\cdot, HS\cdot, S\cdot, H\cdot$) formed by the cleavage of weaker bonds. At this transition state (Fig. 10b), the radical sites may be terminated by abstraction of hydrogen from neighboring molecules, especially molecular hydrogen, which will return the transition molecule to its original state (Fig. 10a). Free radical sites that are not immediately terminated in the transition state may undergo either thermal cracking (Fig. 10c) or cross linking (Fig. 10d). Thermal cracking results in the formation of lower-molecular-weight molecules through β -scission of the carbon-carbon bonds adjacent to the free-radical sites. The resulting cleaved molecular free-radical fragments may undergo either further β -scission to form smaller molecules, termination by abstracting hydrogen from other molecules to propagate the reaction, or termination by

formation of a double carbon bond. The latter termination results in the formation of alkenes, which are common products in open-system pyrolysis. However, the scarcity of alkenes in the products from closed-system pyrolysis under hydrous and anhydrous conditions at 300 to 350°C for 72 h suggests they are neither a significant reaction product nor intermediates in the formation of alkanes. With double-bond formation not being a significant termination reaction in closed-system pyrolysis, an exogenous source of hydrogen is essential to the generation of hydrogen-saturated molecules by the thermal cracking pathway (Fig. 10c).

Conversely, hydrogen is generated when free-radical sites undergo the cross-linking pathway (Fig. 10d). Cross linking involves termination of a free-radical site by formation of a covalent bond between the free-radical carbon and an adjacent intra- or inter-molecular carbon. This reaction pathway is considered responsible for reductions in the amounts of tar and extractable products generated from pyrolyzed coals (Sunberg et al., 1987; Solomon et al., 1990), and for reduced oil yields from pyrolyzed oil shale (Weitkamp and Gutberlet, 1970). That cross linking can occur at low temperatures is demonstrated by irradiation of alkanes. The high free-radical activity induced by radiation results in alkanes becoming infusible and insoluble at 70°C because of cross linking (Charlesby, 1954, 1960). The lower total-pyrolysate yields from anhydrous pyrolysis relative to hydrous pyrolysis of the Woodford Shale at 330 and 350°C after 72 h (Table 2) indicates that in the absence of liquid water, cross linking is promoted and thermal cracking is retarded within the bitumen network of the rock. This preference for the cross-linking pathway in anhydrous pyrolysis is also reflected in the lower hydrogen indices and higher production indices from Rock-Eval pyrolysis of the recovered rocks (Table 3) and lower atomic H/C ratios of the kerogens (Table 4).

The differences in molecular composition (Table 5) of composited pyrolysates from hydrous pyrolysis and bitumens from anhydrous pyrolysis may also be related to the reactions presented in Fig. 10. However, the lack of absolute concentrations makes the assignment of specific reactions to the relative changes in ratios equivocal. As an example, the more condensate-like character (nC_{15}/nC_{25}) and lower n -alkane/isoprenoid ($nC_{17}/\text{pristane}$) ratio of the bitumens from anhydrous pyrolysis may be interpreted as a result of enhanced free-radical quenching (Fig. 10a,b) in hydrous pyrolysis or enhanced cross linking (Fig. 10d) in anhydrous pyrolysis. Initially, the former may be considered more likely because of the preponderance of high-temperature/low pressure pyrolysis studies that emphasize cracking, but the latter may be more likely at lower temperatures and higher pressures. Radiation experiments at low temperatures (i.e., 70°C) have shown that the susceptibility of alkanes to cross linking increases significantly as their carbon number and degree of branching increases (Chapiro, 1962). The other molecular ratios (Table 5) also indicate higher thermal maturities under anhydrous conditions, but interpretation of specific mechanisms responsible for their relative changes will require more quantitative data related to absolute concentrations.

The simple reactions presented in Fig. 10 show that the availability of hydrogen is critical in determining which of these two pathways dominate. With no exogenous source of

hydrogen, two cross-linking reactions are needed to supply the balance of hydrogen needed for one thermal-cracking reaction. Conversely, with an exogenous source of hydrogen, formation of the transition state (Fig. 10b) and cross linking (Fig. 10d) are retarded and thermal cracking is promoted (Fig. 10c). The ability of an exogenous source of hydrogen to promote the thermal cracking pathway and impede the cross-linking pathway has been demonstrated by the enhancement of liquid products and reduction of char products in coal liquefaction and oil-shale retorting with increasing additions of molecular hydrogen (Bockrath et al., 1987; Wen and Kobylinski, 1983; Hershkowitz et al., 1983; Vernon, 1980). The importance of hydrogen is also demonstrated in the gallium-alloy experiment 14 in which the oxidation of gallium by water vaporized from the rock pores generated a high concentration of molecular hydrogen. The total pyrolysate (gas + oil + bitumen) from this experiment was intermediate to those obtained from hydrous pyrolysis and anhydrous pyrolysis at the same experimental conditions (Table 12). The lack of any significant increase in total-pyrolysate yield during hydrous pyrolysis with the addition of 1.48 MPa of molecular hydrogen in the head-space of the reactor suggests that in the presence of liquid water the system is fully saturated with hydrogen and that additional molecular hydrogen has no effect (Table 11, experiment 17).

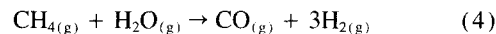
Although the cross-linking reactions generate sufficient hydrogen in anhydrous pyrolysis to ensure that alkene formation does not occur, they do not generate sufficient hydrogen to enhance thermal-cracking reactions in the formation of an expelled oil as observed in hydrous pyrolysis. Table 7 shows that at 350°C after 72 h there is twice as much molecular hydrogen in the anhydrous pyrolysis than in the hydrous pyrolysis, despite the greater total pyrolysate yield in the latter. This excess of molecular hydrogen in anhydrous pyrolysis suggests that hydrogen generated by cross linking occurs too late in the reaction series to enhance thermal cracking. The need of an exogenous source of hydrogen to retard cross linking, the generation of excess oxygen in the form of CO₂, and the high degree of hydrocarbon deuteration in D₂O pyrolysis experiments all indicate that water is an exogenous source of hydrogen that is critical to the thermal decomposition of bitumen to oil.

4.4. Water-Derived Hydrogen

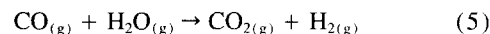
Before discussing mechanisms by which water can act as a source of hydrogen, it is important to emphasize that the reactions take place within the rock chips where water occurs as dissolved molecules within the bitumen network. The bulk liquid water surrounding the rock chips may act as a reservoir to ensure the bitumen is always saturated with dissolved water, but its role as a reactant appears to be insignificant based on the results from experiments 12 and 16 (Table 11). In addition, the mineral matrix of the rock does not appear to play a significant role in the reactions as shown by the similar pyrolysate yields from the isolated-kerogen experiment (Table 13, experiment 18). The similar high concentrations of CO₂ generated in this experiment (Table 14, experiment 18) also indicates that the mineral matrix is not respon-

sible for the excess oxygen needed to account for the CO₂ generated under hydrous conditions. Therefore, in addition to being the source of hydrogen, water is also a source of excess oxygen in the form of CO₂.

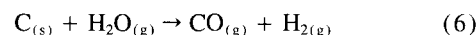
Steam-methane reactions such as the



and the water-gas shift reaction

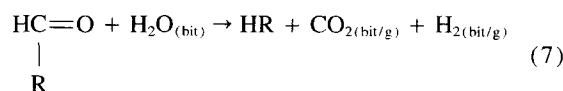


yield CO, CO₂, and H₂ from the interaction of water vapor with methane and carbon monoxide gases. Reaction 4 is not likely during hydrous pyrolysis because it is only operative at 650 to 900°C over a nickel catalyst (Comley and Reed, 1963) and is thermodynamically not possible at temperatures below 627°C (Wagman et al., 1945). Reaction 5 is thermodynamically possible at 350°C (Wagman et al., 1945), but as shown in Table 6, the similar low concentrations of CO in both hydrous and anhydrous experiments at 350°C indicate sufficient quantities of CO are not generated for this reaction to be a significant source of H₂. Another related reaction sequence involves graphite,

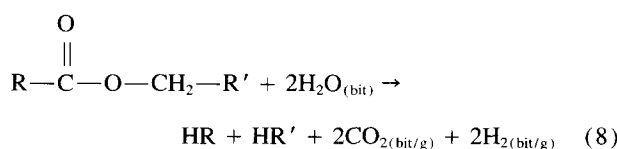


followed by the water-gas shift reaction (reaction 5). Collectively, these two reactions may occur at temperatures as low as 227°C with the aid of a catalyst (Cabrera et al., 1982), but uncatalyzed conditions require temperatures in excess of 900°C for initiation of reaction 6 (Yates and McKee, 1981). Although thin carburized layers (<3.9 μm) of graphitic carbon on reactor-wall surfaces are in contact with water vapor during hydrous pyrolysis, comparison of gases generated in carburized and fresh-metal reactors show no significant differences in amounts of generated CO₂ and H₂ (Lewan, 1993a, Table 5). An additional concern in calling upon water-gas reactions to provide an exogenous source of hydrogen in hydrous pyrolysis is the occurrence of these gas reactions in the head-space of the reactor, rather than within the rock chips. As demonstrated in experiment 17, the addition of H₂ gas in the head-space of the reactor had no significant effect on the pyrolysate yields under hydrous conditions (Table 11, Fig. 7).

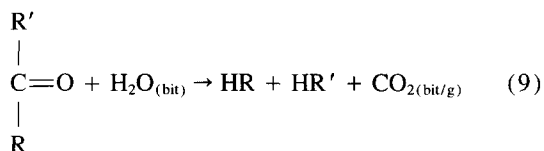
Reactions more likely to be responsible for excess oxygen generated as CO₂ and exogenous hydrogen in the hydrous pyrolysis experiments involve the interaction of dissolved water molecules with carbonyl groups in the bitumen. These reactions may involve aldehydes:



esters:



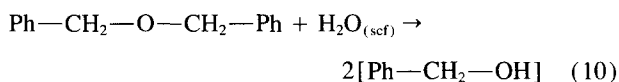
or ketones:



where R and R' are alkyl or aryl groups in bitumen molecules and the *bit* subscript refers to species dissolved in bitumen (i.e., *bituminous phase*). The interaction of water with carbonyl groups has been suggested to be responsible for increased CO₂ concentrations associated with the weathering of coal in water vapor at low temperatures (150°C; Peitt, 1991) and the noncatalytic liquefaction of water-treated coals at 350°C (Song et al., 1994). Reactions 7, 8, and 9 provide one mole of water-derived oxygen for every mole of carbonyl oxygen in the bitumen to form one mole of CO₂. Aldehydes and esters in reactions 7 and 8 also generate one mole of molecular hydrogen for every mole of CO₂ generated. Robin and Rouxhet (1978) report the progressive loss of carboxylic-acid groups, ester groups, and carbonyl groups (ketones and aldehydes) from Type-II kerogens with increasing thermal stress. Their results indicate that carboxylic-acid groups are less thermally stable than ester groups, which are less thermally stable than carbonyl groups. The trace amounts of water vapor in the anhydrous experiments excludes carbonyl and ester groups as major sources of CO₂ by reactions 7 and 8, and limits the source of CO₂ to decarboxylation of carboxylic-acid groups. This more thermally labile and limited source of CO₂ in the anhydrous pyrolysis experiments is supported by the majority of the CO₂ being generated at 300 and 330°C (experiments 2 and 4 with 14.4 and 20.9 mmol, respectively), with only a minor increase in CO₂ generation (i.e., 0.68 mmol) from 330 to 350°C (experiments 4 and 6, Table 7). Decarboxylation of carboxylic-acid groups is also a likely source of CO₂ under hydrous conditions, but the significance of this source may be reduced by preferential generation of aliphatic carboxylic acids, which have been reported in hydrous pyrolysis experiments (Lewan and Fisher, 1994; Barth et al., 1987; Eglinton et al., 1987; Lundegard and Senftle, 1987; Cooles et al., 1987; Kawamura and Ishiwatari, 1985). Assuming that all of the CO₂ generated in the anhydrous experiments is from carboxylic acid groups, an oxygen mass balance may be recalculated on the basis of water contributing one oxygen atom for every CO₂ molecule generated. At 350°C, the total CO₂ difference between hydrous and anhydrous experiments is 219 mmole (Table 7). If this amount of oxygen is derived from ester and carbonyl groups in the kerogen that react with dissolved water, then the oxygen balance (ΔO) reported in Table 8 becomes a surplus of +45 mmol instead of the deficit of -174 mmole. Most of the surplus 45 mmol can be accounted for by the additional 41 mmol of oxygen that occurs in the CO₂ dissolved in the bitumen and oil (~8 mmol) and in the aqueous carboxylic acids (~33 mmol). The 219 mmol of oxygen in carbonyl and ester groups of the kerogen represents approximately 32% of the total oxygen in the original unheated kerogen. This value is reasonable in comparison to published carbonyl- and ester- oxygen contents in immature Type-II kerogens of 34 to 60% (Behar

and Vandembroucke, 1987; Tissot and Welte, 1984). The amount of water-derived hydrogen generated along with these oxidation and decarbonylation reactions is more difficult to approximate because of the lack of information on the relative proportionality between ketone and aldehyde groups in immature Type-II kerogens. However, an estimate of 518 mmol of water-derived hydrogen can be made by assuming all of the excess oxygen in CO₂ and carboxylic acids (i.e., 259 mmol) is derived from the oxidation of ester and aldehyde groups (reactions 7 and 8, respectively).

In addition to water reacting with carbonyl groups, alkyl carbons adjacent to ether linkages react with supercritical water to form alcohols (Townsend et al., 1988). The reaction of dibenzyl ether with supercritical water (*scf*) at 374°C yields benzyl alcohol as a major product:



Although no molecular hydrogen or CO₂ is released from this reaction, the results demonstrate that water molecules may directly interact with alkyl carbons associated with oxygen bonds despite the high bond-dissociation energies of hydrogen-oxygen bonds of water (119 and 102 kcal/mol, Sanderson, 1976). Helgeson et al. (1993) have taken this a step further by arguing from a thermodynamic view that water may directly react with alkyl carbons irrespective of neighboring oxygen atoms. They contend that alkanes with nine or less carbon atoms can react with water under reservoir conditions in the subsurface (i.e., ~100 to 150°C and 40 MPa) to form CO₂ and alkanes with one less alkyl group:



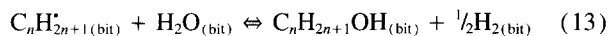
Although it is difficult to envisage the mechanism by which 25 nonane molecules come together in the appropriate alignment with two water molecules to generate 28 octane molecules in this theoretical reaction, the reaction does provide excess oxygen in the form of CO₂ and an exogenous source of hydrogen from water.

An alternative to reaction 11 is the direct reaction of dissolved water molecules with free-radical sites on alkyl groups:



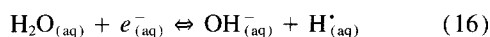
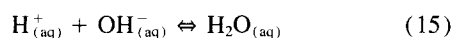
This reaction involves oxygen from a water molecule reacting with an unpaired electron at an alkyl radical site to form an aldehyde and hydrogen. The hydrogen would be available to react with other free radical sites and the aldehyde would react with other water molecules to form a carboxylic acid or CO₂. Each molecule of water that reacts with a free radical site by this reaction, generates three atoms of hydrogen that can terminate or initiate additional free radical sites. A subsequent reaction of the resulting aldehyde with other water molecules yields two additional hydrogen atoms by reaction 7. Therefore, these reactions may collectively generate 5 hydrogen atoms for every water-derived oxygen that reacts with a free radical site. Available thermodynamic data on the constituents of reaction 12 in the vapor phase for *n* = 2 (Benson, 1976; Gurvich et al., 1994) indicate the reaction is thermodynamically favorable between 27 and

374°C (100 kPa) with Gibbs free energies for reaction of -10.5 and -13.5 kcal/mol, respectively. That this reaction does occur in an aqueous phase has been demonstrated experimentally by converting ethene to ethane in aqueous solution at 325°C and 35 MPa (Seewald, 1994). Other thermodynamically favorable water/free radical reactions include

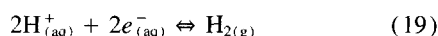


Available thermodynamic data on the constituents of reactions 13 and 14 in the vapor phase for $n = 2$ (Benson, 1976; Gurvich et al., 1994) indicate the reactions are thermodynamically favorable. Gibbs free energies for reaction at 27 and 374°C (100 kPa) are, respectively, -18.8 and -11.9 kcal/mol for reaction 13 and -27.3 and -17.8 kcal/mol for reaction 14. The water-derived oxygen in the alcohol and molecular oxygen released from these reactions may finally occur as carbonyls, carboxyls, or CO_2 through a series of intermediate reactions. Molecular oxygen from reaction 14 would be highly reactive and prone to generate or terminate other free radical sites. Alcohols have not been reported in the products of hydrous pyrolysis experiments, but Stalker et al. (1994) have reported the generation of phenols from water-derived oxygen in $H_2^{18}O$ -experiments with kerogen at 300°C after 72 h. The intent here is not to advocate reactions 12, 13, and 14 as specific reactions in petroleum formation; they simply serve to demonstrate that mechanistically simple reactions between alkyl free-radical sites and water are thermodynamically favorable at standard state conditions and feasible during petroleum formation.

The ability of H_2O liquid to under go heterolytic cleavage to form H^+ and OH^- suggests that protons under reducing conditions may act as another exogenous source of hydrogen through the following series the reactions (Hostettler, 1984; Appendix)



This reaction series reduces to the overall reaction



which is used to describe the stability of H_2O under reducing conditions in the presence of molecular hydrogen gas (Hostettler, 1984). The occurrence of reaction 19 within the hydrous experiments can be evaluated in part by applying measured Eh and pH values to the Nernst equation:

$$Eh = E^0 + (RT/nF) \ln \{ f_{H_2}/[H^+]^2 \}$$

where E^0 is the standard electrode potential, R is the ideal gas constant, T is temperature in Kelvin, n is the number of transferred electrons, F is the Faraday constant, f_{H_2} is the fugacity of molecular hydrogen gas within the reactor (Table 7), and $[H^+]$ is the activity of aqueous hydrogen ions as determined by pH measurements (Table 7). At a room temperature of 25°C, the calculated Eh values are -0.33 volts

for the water recovered from the 300°C experiment 1 and -0.41 volts for the water recovered from the 350°C experiment 5. The measured Eh values at room temperature are -0.37 volts for the water recovered from the 300°C experiment 1 and -0.40 volts for the water recovered from the 350°C experiment 5. Although the gas phase from the reactor was removed before measuring the Eh and pH of the recovered waters at room temperatures, similarities between the calculated and measured Eh values indicate that the water surrounding the rock within the reactor is in equilibrium with the coexisting molecular hydrogen gas and that additional hydrogen is added to the system through the reduction of water. Assuming equilibrium between atmospheric CO_2 (i.e., $10^{-3.5}$ atm) and the water added to the reactors at the beginning of the hydrous experiments, the original pH of the water would be 5.65 (Butler, 1982). Therefore, assuming no exogenous sources of OH^- ions at 350°C in experiment 5, only 7×10^{-4} mmol of H^+ is consumed by reaction 19, based on the final pH of 7.18 for the recovered water. The unlikelihood that H^+ or an ionic mechanism plays a significant role in providing an exogenous source of water-derived hydrogen in petroleum formation is also supported by the lack of any significant change in products when the initial H^+ activity of the added water was increased five orders of magnitude to a pH of 1.0 in experiment 16 (Table 11). Additional support comes from hydrous pyrolysis experiments conducted on kerogen by Stalker (1994), which showed that no significant differences in degree of deuteration and amounts of alkanes generated occurred from pyrolyzed kerogen in D_2O or D_2O plus 0.5 mmol HCl at 315°C for 72 h.

Regardless of the specific mechanism by which water-derived hydrogen is generated, oil, bitumen, and kerogen molecules are likely to have several water-derived hydrogens where terminated free-radical sites prevented β -scission or cross linking. This process would be essentially random, but some preferences may be influenced by differences in the strengths of specific H—C bonds (i.e., primary > secondary > tertiary). This scheme would explain the high degree of deuteration of the kerogen, bitumen, and oil in the D_2O experiment 13, with each deuterated site representing a free radical site that was quenched by D_2O -derived deuterium. This process would be in agreement with the conclusion made by Ross (1992) that deuteration of the shale-derived alkanes from the D_2O experiments by Hoering (1984) indicate multiple exchanges occurred at essentially the same time and at different sites along the same alkane chain. Therefore, deuteration is not limited to sites where C—C bond cleavage occurs, but can also occur where hydrogen abstraction from an alkyl carbon generates a free radical site. The relatively low degree of deuteration to the added pure hydrocarbons (i.e., n -docosane and 1-octadecene) in the molecular probe experiments of Hoering (1984) may be explained in part by the compounds not experiencing the same free-radical field that occurs within the shale bitumen as it decomposes to an immiscible oil.

4.5. Oil Vs. Bitumen

In addition to providing an exogenous source of hydrogen, water also appears to play an important role in expelling a

saturate-enriched oil into the surrounding water from a polar-enriched bitumen that impregnates the rock. These two distinct phases have long been recognized in nature (Louis and Tissot, 1967), with their compositional differences best illustrated in saturate-aromatic-polar (i.e., resins + asphaltenes) ternary diagrams. This type of diagram in Fig. 11a shows the distinct compositional difference between natural crude oils and bitumens extracted from their source rocks. Despite the slightly higher polar content of bitumens and oils generated by hydrous pyrolysis relative to natural crude oils and bitumens, Fig. 11b shows that these two distinct phases are simulated by hydrous pyrolysis experiments. Explaining the separation of these two phases is not a simple task when one realizes that oils and bitumens from nature and hydrous pyrolysis experiments are mutually soluble with one another. Furthermore, no analytical method (e.g., chromatography or molecular sieves) currently known makes a separation of phases with these two different compositions once oil and bitumen are combined. Explanations for the separation of these two phases include preferential sorption of minerals and organic matter, gas stripping, selective dissolution by water, and phase immiscibility.

Anhydrous open- and closed-pyrolysis experiments have demonstrated that minerals can affect the amounts and molecular-weight distributions of hydrocarbons generated from the same kerogen (Espitalie et al., 1980, 1984; Horsfield and Douglas, 1980; Huizinga et al., 1987). However, none of these experimental studies have shown how the amount or type of mineral matter can cause the compositional differences between extracted bitumen and expelled oil as shown in Fig. 11. In addition, experiment 18 shows that hydrous pyrolysis of isolated kerogen yields the same amount of expelled oil and extractable bitumen as hydrous pyrolysis of the kerogen embedded in its natural rock matrix (Table 13). Although preferential sorption of polars by minerals does not appear to be a significant factor in explaining the compositional differences between oil and bitumen, some petroleum expulsion models consider preferential sorption of polars by kerogen a significant factor. Sandvik et al. (1991) presented a descriptive model to account for the compositional differences between expelled oil and bitumen on the basis of preferential retention of polars by kerogen within a source rock. Although this descriptive model can be formulated to give expelled oil and bitumen compositions similar to, but higher in saturates (Sandvik et al., 1991, Fig. 9) than those observed in Fig. 11, the experimental results reported by Lafargue et al. (1989) do not support the main premise that kerogen preferentially retains polars within a source rock. A representative experiment from this study involves two heating steps. First, bitumen was generated in a core of Toarcian source rock by heating it under anhydrous conditions at 300°C and 100 MPa for 48 h. After the core was sampled to determine the composition of the generated bitumen within the rock, the core was again heated under anhydrous conditions at 130°C for 72 h with a confining pressure of 200 MPa. Bitumen that was squeezed into an adjacent air-filled, fritted-metal reservoir during this second heating/squeezing step was collected to determine its composition. Despite the severity of these conditions, which represent lithostatic pressures at subsurface depths approaching 9 Km,

no significant compositional difference was observed between the retained and expelled bitumen as formulated by Sandvik et al. (1991) or observed in hydrous pyrolysis and nature (Fig. 11b).

Another explanation for the compositional difference between expelled oil and bitumen is that gases generated within a source rock strip out a saturate-enriched phase from the bitumen. As these carrier gases are released from the rock, their partial dissolution into and migration through the surrounding water releases the stripped components, which accumulate on the water surface as an expelled oil. An important implication of this explanation is that the water surrounding the rock chips in hydrous pyrolysis acts only as a collection medium for the expelled oil. Results from experiment 14, in which a Ga-In alloy liquid was used instead of water, indicate that while gas stripping is not a significant process, water is a significant part of the process responsible for the separation of oil and bitumen. Excess molecular hydrogen generated by the oxidation of gallium by minor amounts of generated water vapor appears to have enhanced the amount of bitumen generated in the experiment. However, this additional bitumen and the higher amounts of generated gas (Table 12) resulted in no expelled oil on the surface of the Ga-In alloy liquid or on the exposed reactor walls. These experimental results indicate that oil expulsion by gas stripping is not an important process and that water is a critical component in generating an expelled oil. Although oil expulsion by gas stripping has been proposed in some geological settings (Leythaeuser and Poelchau, 1991), experimental work by Price et al. (1983) indicate that only condensates with more than 85 wt% saturates are a likely result of this process and relatively high concentrations of generated gas are needed.

Selective dissolution of a saturate-enriched oil by the water surrounding the rocks during the experiments is also not a viable explanation. Experimental data by Price (1981) indicate that some expelled oil may dissolve in the surrounding water during hydrous pyrolysis experiments. However, the amounts of expelled oil recovered from hydrous experiments (e.g., experiments 2 and 5) exceed the amounts of oil in the C₁₄-C₂₀ distillation fraction that can be dissolved by factors greater than 6. This oversaturation of expelled oil in the surrounding water phase during the hydrous pyrolysis experiments is also confirmed by the observation that an expelled-oil layer formed a char band around a borosilicate-glass liner at the expanded water level in an experiment conducted at 330°C for 72 h (Lewan, 1993a). Additional support for the inability of selective aqueous dissolution to account for the separation of oil and bitumen phases is found in the results from experiment 15, which employed a 5 wt% NaCl solution. If aqueous dissolution was a critical factor in hydrous pyrolysis, the amount of expelled oil in this experiment should have decreased proportionally with the twofold decrease in oil solubility that is observed for 5 wt% NaCl solutions (Price, 1981). The results from this experiment (Table 11) show no decrease in yield, but an increase in amount of expelled oil. Although this increase in yield is not understood, it clearly demonstrates that selective aqueous dissolution is not a significant factor in hydrous experiments. Additional evidence against selective aqueous dissolution is

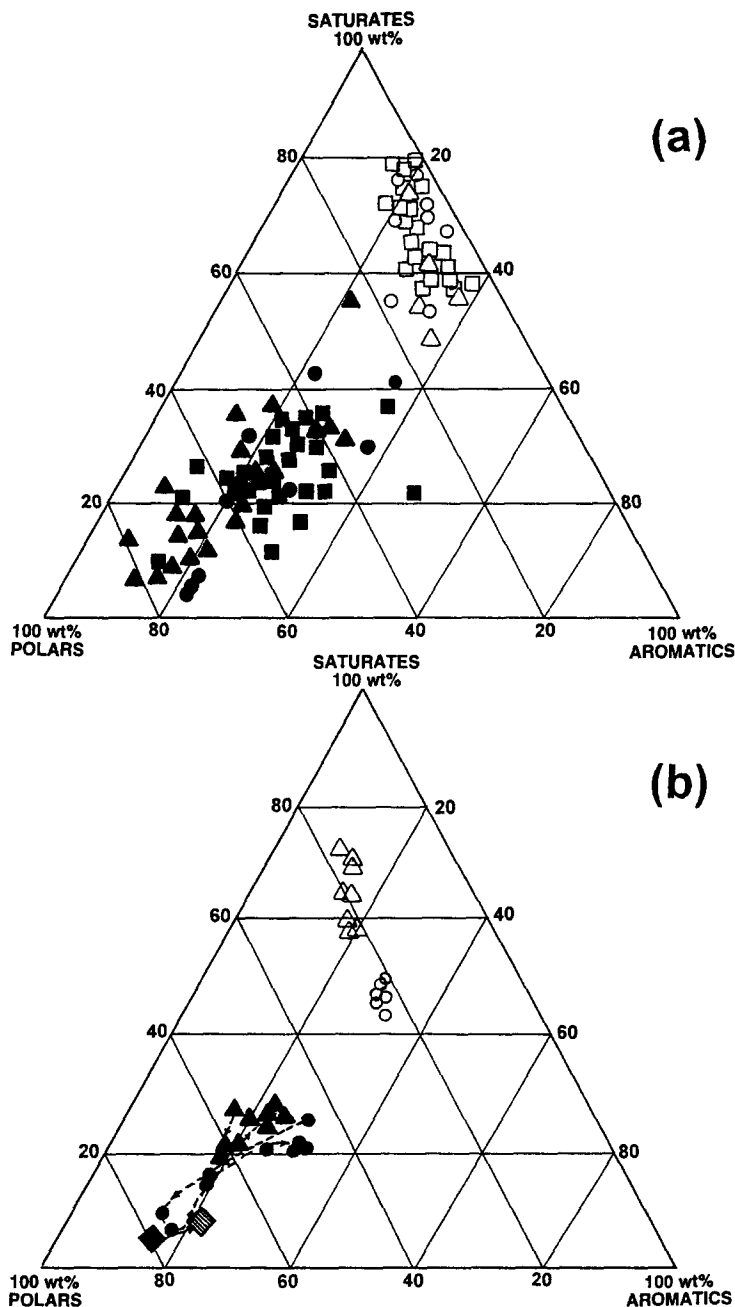


Fig. 11. Gross composition of expelled oils and extracted bitumens plotted on saturate-aromatic-polar ternary diagrams. The polar component includes resins and asphaltenes unless otherwise noted. (a) Ternary plot of natural crude oils (open symbols) and bitumens extracted from their identified source rock (solid symbols). The natural data plotted in this diagram are of Jurassic oils and bitumens from the Parentis basin, France (triangles; Deroo, 1971), Neogene oils and bitumens from the Mahakam delta, Borneo (squares; Combaz and de Matharel, 1978), and Carboniferous/Devonian oils and bitumens from the Dniper-Donets basin, Ukraine (circles; J. L. Clayton and T. E. Ruble pers. commun.). (b) Ternary plot of expelled oils (open symbols) and extracted bitumens (solid symbols) generated by hydrous pyrolysis of the Woodford Shale (circles; Lewan, 1993a; 300 to 365°C for 72 h) and Mahogany Shale (triangles; Ruble, 1996; 270 to 365°C for 72 h). Asphaltenes were not precipitated from the Woodford oils and bitumens prior to column chromatography, and therefore, some asphaltenes may not have completely eluted with the polar component. Diamond symbols denote anhydrous pyrolysis experiments conducted on an immature Toarcian shale, Paris basin (Lafargue et al., 1989). The solid-diamond symbol represents the composition of the bitumen extracted from the shale after it was heated without water at 300°C and 100 MPa for 48 h. The hatched-diamond symbol represents the bitumen expelled from the previously heated shale (i.e., 300°C at 100 MPa for 48 h) after being subjected to a confining pressure of 200 MPa at 130°C for 72 h.

the lack of an increase in expelled oil with a threefold increase in the water:rock ratio of experiment 13 (Table 11).

A more likely explanation for the role of water in separating bitumen and oil phases is that saturate-enriched oil becomes immiscible in the H₂O-saturated, polar-enriched bitumen from which it originates. Figure 9 shows that the solubility of H₂O in polar organic liquids (e.g., glyceride-rich oils) is significant and suggests that more H₂O dissolves in the bitumen phase than in the expelled oil phase. As oil is generated from the thermal decomposition of the H₂O-saturated bitumen, the more saturate-enriched and hydrophobic oil becomes immiscible in the more polar-enriched and hydrophilic bitumen. Experiment 18 (with isolated kerogen) shows that despite the mutual solubility of bitumen and oil under anhydrous conditions, they separate into two distinct phases in the presence of water. The oil phase accumulates on the water surface and the bitumen phase remains submerged in the water with the residual kerogen. An example of water causing an organic solute to become immiscible with an organic solvent is found in cholesterol-triolein solutions. Jandacek et al. (1977) showed that low concentrations of dissolved water (<0.1 wt%) reduced the solubility of cholesterol in triolein by 32%. This reduction in solubility causes precipitation of an immiscible cholesterol-monohydrate phase from the water-saturated glyceride oil. This phenomenon has not been previously considered in petroleum expulsion and remains a fertile area for future research concerning petroleum expulsion from source rocks.

4.6. Geochemical Implications

The role of water as a source of hydrogen and as an essential component in oil expulsion has several important geochemical implications regarding natural petroleum formation in sedimentary basins. The first implication centers on the observation that an exogenous source of hydrogen from water dissolved in the bitumen of a source rock retards the thermal destruction of hydrocarbons by quenching free radical sites before they can initiate thermal-cracking and cross-linking reactions. As a result, the thermal stability field for hydrocarbons can be extended to greater depths within sedimentary basins. This stabilizing effect of water has also been observed in experiments by Hesp and Rigby (1973), in which the thermal destruction of a crude oil to gas was reduced by one order of magnitude in the presence of water at 375°C. Similarly, Arca et al. (1987) observed that the activation energy for thermal destruction of poly(pyrrole) was enhanced by a factor of two when trace amounts of water were present in thermogravimetric experiments up to 700°C. Price (1993) has also recognized the stabilizing effect of water on hydrocarbons and has proposed that the presence of water can account for the preservation of trace quantities of hydrocarbons (i.e., <2000 ppm) in rocks at advanced stages of thermal maturation (i.e., %R₀ > 3.0). These observations suggest that the amount of water available to a source rock can influence the rate its bitumen decomposes to oil or pyrobitumen and the rate its generated oil decomposes to gas or pyrobitumen. Therefore, the utility of kinetic parameters determined under anhydrous conditions for oil generation (e.g., Ungerer and Pelet, 1987; Braun

et al., 1991) and destruction (e.g., Kuo and Michael, 1994; Horsfield et al., 1991) may need further evaluation.

The second implication involves the net volume increase within a source rock that results from the phase separation of oil from a water-saturated bitumen. This volume increase, along with the increase associated with thermal cracking reactions may explain the volume increases observed in hydrous pyrolysis experiments. Lewan (1987) has reported expansion of source-rock cores along *en echelon* partings that open parallel to the bedding fabric after hydrous pyrolysis. These partings contain oil droplets which suggest that oil generation was responsible for their opening. Tentative calculations on the significance of volume increases of organic matter for primary migration (e.g., Ungerer et al., 1983) have not considered the volume changes associated with the uptake of porewater as a dissolved component in the bitumen of a source rock, or the phase separation of oil from water-saturated bitumen. These additional untested causes of a net volume increase in organic matter, which are observed in hydrous pyrolysis experiments, may provide a more viable mechanism for oil expulsion and the overpressuring of maturing source rocks. A more viable mechanism is needed especially because the mechanism envisaged by Ungerer (1993) in which significant quantities of oil are squeezed out of source rocks with burial compaction is supported neither by laboratory experiments (Lafargue et al., 1989) nor porosity losses in naturally compacted fine-grained rocks (Hunt, 1996).

The third implication relates to the effect the amount of water dissolved in bitumen has on generating expelled oil. Water solubilities in bitumen at the higher temperatures used in hydrous pyrolysis are an order of magnitude higher than those at the lower temperatures experienced in sedimentary basins. These higher concentrations of dissolved water in hydrous pyrolysis would provide more exogenous hydrogen to minimize cross-linking reactions and more dissolved water to the bitumen to maximize the formation of immiscible oil. As a result, it is expected that the amounts of expelled oil generated by hydrous pyrolysis will be exaggerated. The degree of exaggeration remains to be determined, but it may be twofold or more as is suggested by a material-balance assessment of petroleum in the Illinois basin (Lewan et al., 1995). This implication is significant because current methods for estimating the amount of oil expelled from a source rock (Cooles et al., 1986) are based on anhydrous open-system pyrolysis, which give calculated yields of expelled oil that are twofold greater than those obtained from hydrous pyrolysis (Lewan, 1994). This exaggeration equates to at least a fourfold overestimation of expelled oil in sedimentary basins (Lewan et al., 1995).

The final implication relates to the high concentration of CO₂ generated by hydrous pyrolysis and the consequences of this gas in a sedimentary basins. Unlike the generated hydrocarbon gases, carbon dioxide is highly soluble in oil and water, and is highly reactive with aqueous and solid inorganic components in sedimentary rocks. Therefore, it is not surprising that CO₂ concentrations are usually low and variable in natural gas accumulations (Franks and Forester, 1984). CO₂ generated from maturing source rocks has been suggested as the source of acid for secondary porosity forma-

tion in sedimentary basins (Schmidt and McDonald, 1979), but mass balance calculations by Lundegard et al. (1984) indicate that there is insufficient oxygen in kerogens to provide the quantities of CO₂ needed. The ability of dissolved water in bitumen of a source rock to oxidize organic components to carboxylic groups suggests that the amount of CO₂ generated from source rocks is not limited to the initial oxygen content of a kerogen as used in some studies (Pittman and Hathon, 1994). This organically derived CO₂ may also serve as a source of ¹³C-depleted carbon in late-stage carbonate cements (e.g., Moore and Heydari, 1993; Dixon et al., 1989; Boles and Ramseyer, 1987; Franks and Forester, 1984; Loucks et al., 1981). In addition, this source of CO₂ is not limited to the early stages of oil generation, as is suggested in some reaction schemes (Tissot and Welte, 1984), but may continue to be generated throughout the oil-generation stage, as shown by the experimental results in this study.

5. CONCLUSIONS

Experimental results from this study indicate that water dissolved in the bitumen of petroleum source rocks plays a chemical and physical role in the generation and expulsion of petroleum. Although dissolved water does not appear to significantly influence the thermal decomposition of kerogen to bitumen through the cleavage of weak bonds, it does have a decisive role in determining the reaction pathway by which covalent bonds within the bitumen thermally decompose. Bitumen decomposition in the presence of water results in the generation and expulsion of a saturate-enriched oil. Bitumen decomposition in the absence of water results in the generation of insoluble organic matter referred to as pyrobitumen. These two different reaction products are explained by two opposing reaction pathways involving thermal cracking and cross linking. Thermal cracking dominates in the presence of water to generate the expelled oil observed in hydrous pyrolysis experiments, and carbon-carbon bond cross linking dominates in the absence of water to generate the pyrobitumen observed in anhydrous pyrolysis experiments. An exogenous source of hydrogen during the thermal decomposition of bitumen is the controlling factor that determines which of these two reaction pathways dominates, with hydrogen being consumed by thermal cracking and generated by cross linking.

Dissolved water within the bitumen provides an exogenous source of hydrogen during hydrous pyrolysis. The availability of this exogenous hydrogen retards the progress of both reaction pathways by quenching free radical sites within the bitumen before cross linking and thermal cracking occur. The high degree of deuterated products (i.e., expelled oil, bitumen, and kerogen) generated in hydrous pyrolysis experiments conducted with D₂O is interpreted to represent the quenching of free radical sites by water-derived hydrogen. When thermal cracking occurs before a free radical site can be quenched, the free radical site generated by the β -scission can be terminated by exogenous hydrogen before cross linking with neighboring carbons occurs. Under anhydrous pyrolysis, cross linking is the only source of hydrogen, which limits the quenching of free radical sites and allows free radical terminations by subsequent cross linking to dominate.

The reaction by which dissolved water in the bitumen of a rock produces hydrogen remains uncertain, but the reaction is accompanied by the generation of excess oxygen in the form of CO₂. Two overall reaction schemes are suggested. The first scheme involves the interaction of dissolved water molecules with existing carbonyl groups in the bitumen to form an exogenous source of hydrogen and carboxyl groups, which decarboxylate at higher thermal stress levels to form CO₂. Observed CO₂ increases associated with coal weathering in water vapor at 150°C and with noncatalytic liquefaction of water-treated coals at 350°C have been attributed to reactions of this scheme. The second scheme involves the direct interaction of dissolved water molecules with free radical sites. These reactions may involve either the oxygen or hydrogen of the water molecule reacting with unpaired electrons to form either allylic hydrogens, carbonyls, or hydroxyls at radical sites. The oxygen and oxygen functional groups produced by this reaction scheme are believed to react with dissolved water according to the first reaction scheme to produce additional hydrogen. Available data on the constituents of these water/radical reactions in the vapor phase indicate that these reactions are thermodynamically favorable at temperatures between 27 and 374°C at 100 kPa. Reduction of the water surrounding the rock chips in the presence of molecular hydrogen occurs in agreement with the Nernst equation, but the amount of exogenous hydrogen generated by this reduction is not significant. In addition, the lack of a significant change in product yields with elevated H⁺ activities indicate that ionic mechanisms are not critical to petroleum formation.

In addition to being a source of hydrogen, dissolved water in the bitumen of a rock is critical to the formation and expulsion of an immiscible oil phase. Pyrolysis on a source rock in the presence of a liquid gallium alloy instead of liquid water produced an exogenous source of hydrogen from the oxidation of gallium by water vapor released from the rock pores. This exogenous hydrogen produced pyrolysate yields intermediate to those from anhydrous and hydrous pyrolysis under the same thermal stress levels. However, an expelled oil phase was not observed on the liquid Ga alloy surface at the end of the experiment, as observed in hydrous experiments. The compositional differences between expelled oils and bitumen extracts generated naturally and by hydrous pyrolysis is one of the most compelling observations that indicate water is critical to petroleum generation and expulsion. No closed-system anhydrous pyrolysis method, including squeezing of pyrolysate from mature source rocks at excessively high pressures (200 MPa), has been able to simulate these compositional differences between oil and bitumen. The ability of hydrous pyrolysis to generate a saturate-enriched oil phase that is immiscible with a polar-enriched bitumen from rocks and their isolated kerogen indicates that preferential sorption of polars by minerals is not significant. Hydrous pyrolysis experiments with varying water:rock ratios and with a 5 wt% NaCl solution indicate that selective aqueous dissolution of a saturate-enriched phase is also not a viable explanation for the two phases. At present, the most plausible hypothesis is that saturate-enriched oil generated from the thermal decomposition of bitumen be-

comes immiscible with the residual bitumen because of its dissolved water content.

The overall geochemical implication of these results is that it is essential to consider the role of water in experimental studies designed to understand natural rates of petroleum generation, expulsion mechanisms of primary migration, thermal stability of crude oil, reaction kinetics of biomarker transformations, subsurface sources of CO₂, and thermal maturity indicators in sedimentary basins. Although the degree to which hydrous pyrolysis exaggerates natural interactions between maturing organic matter and water in sedimentary basins remains to be determined, the ubiquity of water and its interaction with organic matter in the subsurface cannot be neglected in developing a complete understanding of petroleum formation.

Acknowledgments—The experiments described in this study were conducted by the author during his employment with Amoco Production Company Research Center. The author thanks Amoco Production Company for supporting this experimental research and for releasing the experimental data for this study and its publication. Constructive comments and suggestions by Drs. Alan Burnham, Robert Burruss, John Curtis, Steve Franks, Robert Olson, Leigh Price, Tim Ruble, Paul Taylor, and an anonymous reviewer helped in revising the original manuscript and are greatly appreciated.

Editorial Handling: J. T. Sentfle

REFERENCES

- Arca M., Arca E., Yildiz A., and Guven O. (1987) Thermal stability of poly(pyrrole). *J. Mater. Sci. Lett.* **6**, 1013–1015.
- Barth T., Borgund A. E., Hopland A. L., and Grave A. (1987) Volatile organic acids produced during kerogen maturation—amounts, composition and role in migration of oil. *Org. Geochem.* **13**, 461–465.
- Barth T., Borgund A. E., and Hopland A. L. (1989) Generation of organic compounds by hydrous pyrolysis of Kimmeridge oil shale—bulk results and activation energy calculations. *Org. Geochem.* **14**, 69–76.
- Baskin D. K. and Peters K. E. (1992) Early generation characteristics of a sulfur-rich Monterey kerogen. *Amer. Assoc. Petrol. Geol. Bull.* **76**, 1–13.
- Behar F. and Vandenbroucke M. (1987) Chemical modelling of kerogens. *Org. Geochem.* **11**, 15–24.
- Beltrame P. L., Carniti P., Audisio G., and Bertini F. (1989) Catalytic degradation of polymers: Part II—Degradation of polyethylene. *Poly. Degrad. Stabil.* **26**, 209–220.
- Benson S. W. (1976) *Thermochemical Kinetics*. Wiley.
- Bockrath B. C., Illig E. G., and Wassell-Bridger W. D. (1987) Solvent swelling of liquefaction residues. *Energy & Fuels* **1**, 226–227.
- Boles J. R. and Ramseyer K. (1987) Diagenetic carbonate in Miocene sandstone reservoir, San Joaquin Basin, California. *AAPG Bull.* **71**, 1475–1487.
- Brady C. J., Cunningham J. R., and Wilson G. M. (1982) Water-hydrocarbon liquid-liquid-vapor equilibrium measurements to 500°F. Gas Processors Association Res. Rept. 62, 66 pp.
- Braun R. L. and Rothman A. J. (1975) Oil-shale pyrolysis: Kinetics and mechanism of oil production. *Fuel* **54**, 129–131.
- Braun R. L., Burnham A. K., Reynolds J. G., and Clarkson J. E. (1991) Pyrolysis kinetics for lacustrine and marine source rocks by programmed micro-pyrolysis. *Energy & Fuels* **5**, 192–204.
- de la Breteque P. (1978) Gallium and gallium compounds. In *Kirk-Othmer Encyclopedia of Chemical Technology*, 3d ed., vol. 2., pp. 604–620. Wiley.
- Brooks B. T. (1952) Evidence of catalytic action in petroleum formation. *Indust. Eng. Chem.* **44**, 2570–2577.
- Brooks J. D. and Smith J. W. (1969) The diagenesis of plant lipids during the formation of coal, petroleum and natural gas—II. Coalification and the formation of oil and gas in the Gippsland Basin. *Geochim. Cosmochim. Acta* **33**, 1183–1194.
- Buchardt B. and Lewan M. D. (1990) Reflectance of vitrinite-like macerals as a thermal maturity index for Cambrian-Ordovician Alum Shale, southern Scandinavia. *Amer. Assoc. Petrol. Geol. Bull.* **74**, 394–406.
- Burnham A. K. and Happe J. A. (1984) On the mechanism of kerogen pyrolysis. *Fuel* **63**, 1353–1356.
- Butler J. N. (1982) *Carbon Dioxide Equilibria and their Applications*. Addison-Wesley.
- Cabrera A. L., Heinemann H., and Somorjai G. A. (1982) Methane production from the catalyzed reaction of graphite and water vapor at low temperatures (500–600K). *J. Catal.* **75**, 7–22.
- Campbell J. H., Koskinas G. H., Stout N. D., and Coburn T. T. (1978) Oil shale retorting: Effects of partial size and heating rate on oil evolution and intrapartical oil degradation. *In Situ* **2**, 1–47.
- Carroll J. J. and Mather A. E. (1989) Phase equilibrium in the system water-hydrogen sulfide: Modelling the phase behavior with an equation of state. *Canadian J. Chem. Eng.* **67**, 999–1003.
- Chapiro A. (1962) *Radiation Chemistry of Polymeric Systems*. Interscience.
- Charlesby A. (1954) The cross-linking and degradation of paraffin chains by high-energy radiation. *Proc. Roy. Soc. London* **222**, 60–74.
- Charlesby A. (1960) *Atomic Radiation and Polymers*. Pergamon.
- Chiantore O., Camino G., Costa L., and Grassie N. (1981) “Weak Links” in polystyrene. *Poly. Degrad. Stabil.* **3**, 209–219.
- Chiantore O., Guaita M., and Grassie N. (1985) Evidence of random chain scissions at low temperatures in the thermal degradation of anionic polystyrenes. *Poly. Degrad. Stabil.* **12**, 141–148.
- Clifford C. W. (1921) The solubility of water in gasoline and in certain other organic liquids, determined by the calcium chloride method. *J. Ind. Eng. Chem.* **13**, 631–632.
- Coburn T. T., Oh M. S., Crawford R. W., and Foster K. G. (1989) Water generation during pyrolysis of oil shales. I. Sources. *Energy & Fuels* **3**, 216–223.
- Combaz A. and de Matharel M. (1978) Organic sedimentation and genesis of petroleum in Mahakam delta, Borneo. *Amer. Assoc. Petrol. Geol. Bull.* **62**, 1684–1695.
- Comet P. A., McEvoy J., Giger W., and Douglas A. G. (1986) Hydrous and anhydrous pyrolysis of DSDP Leg 75 kerogens—A comparative study using a biological marker approach. *Org. Geochem.* **9**, 171–182.
- Comley E. A. and Reed R. M. (1963) Catalytic processes for hydrogen manufacturing. *Sixth World Petrol. Congr.* **4**, 361–372.
- Connan J. (1974) Time-temperature relation in oil genesis: *Amer. Assoc. Petrol. Geol. Bull.* **58**, 2516–2521.
- Cooles G. P., Mackenzie A. S., and Quigley T. M. (1986) Calculation of petroleum masses generated and expelled from source rocks. *Org. Geochem.* **10**, 325–245.
- Cooles G. P., Mackenzie A. S., and Parkes R. J. (1987) Non-hydrocarbons of significance in petroleum exploration: Volatile fatty acids and non-hydrocarbon gases. *Mineral. Mag.* **51**, 483–493.
- Cummins J. J. and Robinson W. E. (1972) Thermal degradation of Green River kerogen at 150° to 350°C. U.S. Bureau of Mines, Investigation Report 7620.
- Deroo G. (1971) Correlations of crude oils and source rocks in some sedimentary basins. *Bull. Centre Rech. Pau-SNPA* **10**, 317–335.
- Dixon S. A., Summers D. M., and Surdam R. C. (1989) Diagenesis and preservation of porosity in Norphlet Formation (Upper Jurassic), southern Alabama. *AAPG Bull.* **73**, 707–728.
- Drever J. I. (1984) *The Chemistry of Weathering*. D. Reidel.
- Drummond S. E. (1981) Boiling and mixing of hydrothermal fluids: Chemical effects on mineral precipitation. Ph.D. dissertation, Pennsylvania State Univ.
- Eglinton T. I., Curtis C. D., and Rowland S. R. (1987) Generation of water-soluble organic acids from kerogen during hydrous pyrolysis: Implications for porosity development. *Mineral. Mag.* **51**, 495–503.
- Engler K. O. V. (1913) *Die Chemie Und Physik Des Erdols.*, vol. 1. S. Hirzel.

- Espitalie J., Madec M., and Tissot B. (1980) Role of mineral matrix in kerogen pyrolysis: Influence on petroleum generation and migration. *Amer. Assoc. Petrol. Geol. Bull.* **64**, 59–66.
- Espitalie J., Makadi K. S., and Trichet J. (1984) Role of mineral matrix during kerogen pyrolysis. *Org. Geochem.* **6**, 365–382.
- Ferry J. M. (1983) Regional metamorphism of the Vassalboro Formation, south-central Maine, USA: A case study of the role of fluid in metamorphic petrogenesis. *J. Geol. Soc. London* **140**, 551–576.
- Fischer F. (1925) *The Conversion of Coal into Oil*. Ernest Benn Ltd.
- Franks S. G. and Forester R. W. (1984) Relationships among secondary porosity, pore-fluid chemistry and carbon dioxide, Texas Gulf Coast. In *Clastic Diagenesis* (ed. D. A. McDonald and R. C. Surdam), pp. 63–79. American Association of Petroleum Geologists, Memoir 37.
- Gavin M. J. (1922) Oil-shale—an historical, technical, and economic study. U.S. Bureau of Mines Bulletin 210, pp. 179–189.
- Garven G., Person M. A., and Sverjensky D. A. (1993) Genesis of stratabound ore deposits in the midcontinent basins of North America. 1. The role of regional groundwater flow. *Amer. J. Sci.* **293**, 497–568.
- Goldstein T. P. (1983) Geocatalytic reactions in formation and maturation of petroleum. *Amer. Assoc. Petrol. Geol. Bull.* **67**, 152–159.
- Greensfelder B. S. and Voge H. H. (1945) Catalytic cracking of pure hydrocarbons. *Indust. Eng. Chem.* **37**, 514–520.
- Griswold J. and Kasch J. E. (1942) Hydrocarbon-water solubilities at elevated temperatures and pressures. *Ind. Eng. Chem.* **34**, 804–806.
- Groschuff E. (1911) The solubility of water in benzene, petroleum, and paraffin oil. *Zeit. Elektrochem.* **17**, 348–354.
- Guerrant R. P. (1964) Hydrocarbon-water solubilities at high temperatures under vapor-liquid-liquid equilibrium conditions. Ph.D. dissertation, Pennsylvania State Univ.
- Gurvich L. V., Iorish V. S., Yungman V. S., and Dorofeeva O. V. (1994) Thermodynamic properties as a function of temperature. In *CRC Handbook of Chemistry and Physics*, 75th ed. (ed. D. R. Lide), pp. 48–71. CRC Press.
- Haas J. L., Jr. (1976) Physical properties of the coexisting phases and thermochemical properties of the H₂O component in boiling NaCl solutions. USGS Bulletin 1421-A.
- Heidman J. L., Tsonopoulos C., Brady C. J., and Wilson G. M. (1985) High-temperature mutual solubilities of hydrocarbons and water. Part II: Ethylbenzene, ethylcyclohexane, and n-octane. *AIChE J.* **31**, 376–384.
- Helgeson H. C., Knox A. M., Owens C. E., and Shock E. L. (1993) Petroleum, oil field waters, and authigenic mineral assemblages: Are they in metastable equilibrium in hydrocarbon reservoirs? *Geochim. Cosmochim. Acta* **57**, 3295–3339.
- Hershey J. P., Plese T., and Millero F. J. (1988) The pK*, for the dissociation of H₂S in various ionic media. *Geochim. Cosmochim. Acta* **52**, 2047–2051.
- Hershkovitz F., Olmstead W. N., Rhodes R. P., and Rose K. D. (1983) Molecular mechanism of oil shale pyrolysis in nitrogen and hydrogen atmospheres. In *American Chemical Society Symposium Series 230* (ed. F. P. Miknis and J. F. McKay), pp. 301–316.
- Hesp W. and Rigby D. (1973) The geochemical alteration of hydrocarbons in the presence of water. *Erdol Kohle-Erdgas-Petrochem. Brennstoff-Chemie* **26**, 70–76.
- Hilder M. H. (1968) The solubility of water in edible oils and fats. *J. Amer. Oil Chem. Soc.* **45**, 703–707.
- Hilder M. H. (1971) The solubility of water in edible oils and fats above 100°C. *J. Amer. Oil Chem. Soc.* **48**, 296–298.
- Ho T. Y., Rogers M. A., Drushel H. V., and Koons C. B. (1974) Evolution of sulfur compounds in crude oils. *Amer. Assoc. Petrol. Geol. Bull.* **58**, 2338–2348.
- Hoering T. C. (1984) Thermal reactions of kerogen with added water, heavy water and pure organic substances. *Org. Geochem.* **5**, 267–278.
- Horsfield B. and Douglas A. G. (1980) The influence of minerals on the pyrolysis of kerogens. *Geochim. Cosmochim. Acta* **44**, 1119–1131.
- Horsfield B., Schenk H. J., Mills N., and Welte D. H. (1991) An investigation of the in-reservoir conversion of oil to gas: Compositional and kinetic findings from closed-system programmed-temperature pyrolysis. *Org. Geochem.* **19**, 191–204.
- Hostettler J. D. (1984) Electrode electrons, aqueous electrons, and redox potentials in natural waters. *Amer. J. Sci.* **284**, 734–759.
- Huizinga B. J., Tannenbaum E., and Kaplan I. R. (1987) The role of minerals in the thermal alteration of organic matter—III. Generation of bitumen in laboratory experiments. *Org. Geochem.* **11**, 591–604.
- Huizinga B. J., Aizenshtat Z. A., and Peters K. E. (1988) Programmed pyrolysis-gas chromatography of artificially matured Green River kerogen. *Energy & Fuel* **2**, 74–81.
- Hunt J. M. (1979) *Petroleum Geochemistry and Geology*. W. H. Freeman.
- Hunt J. M. (1996) *Petroleum Geochemistry and Geology*, 2nd ed. W. H. Freeman.
- Hunt J. M., Lewan M. D., and Hennes R. J.-C. (1991) Modeling oil generation with time-temperature index graphs based on the Arrhenius equation. *Amer. Assoc. Petrol. Geol. Bull.* **75**, 795–807.
- Jandacek R. J., Webb M. R., and Mattson F. H. (1977) Effect of an aqueous phase on the solubility of cholesterol in an oil phase. *J. Lipid Res.* **8**, 203–210.
- Jurg J. W. and Eisma E. (1964) Petroleum hydrocarbons: Generation from fatty acids. *Science* **144**, 1451–1452.
- Kawamura K. and Ishiwatari R. (1985) Behavior of lipid compounds on laboratory heating of a recent sediment. *Geochem. J.* **19**, 113–126.
- Kerr R. A. (1994) German super-deep hole hits bottom. *Science* **266**, 545.
- Kirchko A. A. and Gagarin S. G. (1990) New ideas of coal organic matter chemical structure and mechanism of hydrogenation processes. *Fuel* **69**, 885–891.
- Kuangzong Q., Qiushui Y., Shaohui G., Qinghua L., and Wei S. (1994) Chemical structure and hydrocarbon formation of the Hunxian brown coal, China. *Org. Geochem.* **21**, 333–341.
- Kuo Lung-Chuan and Michael G. E. (1994) A multicomponent oil-cracking kinetics model for modeling preservation and composition of reservoir oils. *Org. Geochem.* **21**, 911–925.
- Lafargue E., Espitalie J., Jacobsen T., and Eggen S. (1989) Experimental simulation of hydrocarbon expulsion. *Org. Geochem.* **16**, 121–131.
- Lewan M. D. (1983) Effects of thermal maturation on stable organic carbon isotopes as determined by hydrous pyrolysis of Woodford Shale. *Geochim. Cosmochim. Acta* **47**, 1471–1479.
- Lewan M. D. (1985) Evaluation of petroleum generation by hydrous pyrolysis experimentation. *Phil. Trans. Roy. Soc. London* **315**, 123–134.
- Lewan M. D. (1986) Stable carbon isotopes of amorphous kerogens from Phanerozoic sedimentary rocks. *Geochim. Cosmochim. Acta* **50**, 1583–1591.
- Lewan M. D. (1987) Petrographic study of primary petroleum migration in the Woodford shale and related rock units. In *Migration of Hydrocarbons in Sedimentary Basins* (ed. B. Doligez), pp. 113–130. Editions Technip.
- Lewan M. D. (1989) Hydrous pyrolysis study of oil and tar generation from Monterey Shale containing high sulfur kerogen. *Amer. Chem. Soc. Natl. Mtg. Abstr.*, April 9–14. Dallas.
- Lewan M. D. (1993a) Laboratory simulation of petroleum formation: Hydrous pyrolysis. In *Organic Geochemistry* (ed. M. H. Engel and S. A. Macko), pp. 419–442. Plenum.
- Lewan M. D. (1993b) Identifying and understanding suppressed vitrinite reflectance through hydrous pyrolysis experiments. 10th Ann. Mtg. Soc. Org. Petrol. Abstr. **10**, pp. 1–3.
- Lewan M. D. (1994) Assessing natural oil expulsion from source rocks by laboratory pyrolysis. In *Amer. Assoc. Petrol. Geol. Mem.* **60** (ed. L. B. Magoon and W. G. Dow), pp. 201–210.
- Lewan M. D. and Buchardt B. (1989) Irradiation of organic matter by uranium decay in the Alum Shale, Sweden. *Geochim. Cosmochim. Acta* **53**, 1307–1322.

- Lewan M. D. and Fisher J. B. (1994) Organic acids from petroleum source rocks. In *Organic Acids in Geological Processes* (ed. E. D. Pittman and M. D. Lewan), pp. 70–114. Springer Verlag.
- Lewan M. D., Winters J. C., and McDonald J. H. (1979) Generation of oil-like pyrolyzates from organic-rich shales. *Science* **203**, 897–899.
- Lewan M. D., Bjoroy M., and Dolcater D. L. (1986) Effects of thermal maturation on steroid hydrocarbons as determined by hydrous pyrolysis of phosphoria retort shale. *Geochim. Cosmochim. Acta* **50**, 1977–1987.
- Lewan M. D., Ulmishek G. F., Harrison W., and Schreiner F. (1991) Gamma ^{60}Co -irradiation of organic matter in the Phosphoria Retort Shale. *Geochim. Cosmochim. Acta* **55**, 1051–1063.
- Lewan M. D. et al. (1995) Feasibility study of material balance assessment of petroleum from the New Albany Shale in the Illinois basin. *USGS Bull.* 2137.
- Leythaeuser D. and Poelchau H. S. (1991) Expulsion of petroleum from type III kerogen source rocks in gaseous solution: Modelling of solubility fractionation. In *Petroleum Migration* (ed. W. A. England and A. J. Fleet); *Geol. Soc. Spec. Publ.* **59**, pp. 33–46.
- Loucks R. G., Richmann D. L., and Milliken K. L. (1981) Factors controlling reservoir quality in Tertiary sandstones and their significance to geopressured geothermal production. Texas Bureau of Economic Geology Report of Investigation No. 111, 41 pp.
- Loucks R. G., Dodge M. M., and Galloway W. E. (1984) Regional controls on diagenesis and reservoir quality in lower Tertiary sandstones along the Texas Gulf Coast. In *Clastic Diagenesis* (ed. D. A. McDonald and R. C. Surdam); *AAPG Memoir* **37**, pp. 15–45.
- Louis M. and Tissot B. (1967) Influence de la temperature et de la pression sur la formation des hydrocarbures dans les argiles a kerogene. *Seventh World Petroleum Congress* **2**, 47–60.
- Lundegard P. D. and Senftle J. T. (1987) Hydrous pyrolysis: A tool for the study of organic acid synthesis. *Appl. Geochem.* **2**, 605–612.
- Lundegard P. D., Land L. S., and Galloway W. E. (1984) Problem of secondary porosity: Frio Formation (Oligocene), Texas Gulf Coast. *Geology* **12**, 399–402.
- Machel H. G. and Mountjoy E. W. (1987) General constraints on extensive pervasive dolomitization—and their application to the Devonian carbonates of western Canada. *Bull. Canadian Petrol. Geol.* **35**, 143–158.
- Madorsky S. L. (1953) Rates and activation energies of thermal degradation of styrene and acrylate polymers in a vacuum. *J. Poly. Sci.* **11**, 491–506.
- Madorsky S. L. (1964) *Thermal Degradation of Organic Polymers*. Interscience.
- Madorsky S. L. and Straus S. (1954) Thermal degradation of polymers as a function of molecular structure. *J. Res. Natl. Bur. Stds.* **53**, 361–370.
- Malhotra S. L., Hess J., and Blanchard L. P. (1975) Thermal decomposition of polystyrene. *Polymer* **16**, 81–93.
- March J. (1985) *Advanced Organic Chemistry*, 3rd. ed. Wiley.
- Minkova V., Razvigorova M., Goranova M., Ljutzkanov L., and Angelova G. (1991) Effect of water vapor on the pyrolysis of solid fuels 1. Effects of water vapor during pyrolysis of solid fuels on yield and composition of the liquid products. *Fuel* **70**, 713–719.
- Monthieux M., Landais P., and Monin J. C. (1985) Comparison between natural and artificial maturation series of humic coals from the Makhakam Delta, Indonesia. *Org. Geochem.* **8**, 275–292.
- Moore C. H. and Heydari E. (1993) Burial diagenesis and hydrocarbon migration in Platform limestones: A conceptual model based on the upper Jurassic of the Gulf Coast of the USA. In *Diagenesis and Basin Development* (ed. A. D. Horbury and A. G. Robinson); *AAPG Studies in Geology* **36**, 213–229.
- Mukdeeprom P. and Edwards J. G. (1987) The isomolecular exchange reaction $\text{GA}_2\text{S}(\text{g}) + \text{IN}_2\text{S}(\text{g}) = 2\text{InGaS}(\text{g})$. *Thermochim. Acta* **112**, 141–149.
- Peitt J. C. (1991) A comprehensive study of the water vapour/coal system: Application to the role of water in the weathering of coal. *Fuel* **70**, 1053–1058.
- Peng D. Y. and Robinson D. B. (1976) A new two-constant equation of state. *Ind. Eng. Chem. Fund.* **15**, 59–64.
- Peters K. E. and Moldowan J. M. (1993) *The Biomarker Guide*. Prentice Hall.
- Peters K. E., Moldowan J. M., and Sundaraman P. (1990) Effects of hydrous pyrolysis on biomarker thermal maturity parameters: Monterey phosphatic and siliceous members. *Org. Geochem.* **15**, 249–265.
- Pittman E. D. and Hathon L. A. (1994) Material balance considerations for the generation of secondary porosity by organic acids and carbonic acid derived from kerogen, Denver basin, Colorado, USA. In *Organic Acids in Geological Processes* (ed. E. D. Pittman and M. D. Lewan), pp. 115–137. Springer-Verlag.
- Poltorak V. A. and Voevodsky V. V. (1969) On the single chain mechanism for the thermal decomposition of hydrocarbons. In *Selected Readings in Chemical Kinetics* (ed. M. H. Back and K. J. Laidler), pp. 171–175. Pergamon.
- Price L. C. (1976) Aqueous solubility of petroleum as applied to its origin and primary migration. *Amer. Assoc. Petrol. Geol. Bull.* **60**, 213–244.
- Price L. C. (1981) Aqueous solubility of crude oil to 400°C and 2,000 bars pressure in the presence of gas. *J. Petrol. Geol.* **4**, 195–223.
- Price L. C. (1993) Thermal stability of hydrocarbons in nature: Limits, evidence, characteristics, and possible controls. *Geochim. Cosmochim. Acta* **57**, 3261–3280.
- Price L. C., Wenger L. M., Ging T., and Blount C. W. (1983) Solubility of crude oil in methane as a function of pressure and temperature. *Org. Geochem.* **4**, 201–221.
- Rettich T. R., Handa Y. P., Battino R., and Wilhelm E. (1981) Solubility of gases in liquids. 13. High-precision determination of Henry's constants for methane and ethane in liquid water at 275 to 328 K. *J. Phys. Chem.* **85**, 3230–3237.
- Rieke H. H., III and Chilingarian G. V. (1974) *Compaction of Argillaceous Sediments*. Elsevier.
- Robin P. L. and Rouxhet P. G. (1978) Characterization of kerogens and study of their evolution by infrared spectroscopy: Carbonyl and carboxyl groups. *Geochim. Cosmochim. Acta* **42**, 1341–1349.
- Ross D. S. (1992) Comments on the source of petroleum hydrocarbons in hydrous pyrolysis. *Org. Geochem.* **18**, 79–81.
- Rouxhet P. G. and Robin P. L. (1978) Infrared study of the evolution of kerogens of different origins during catagenesis and pyrolysis. *Fuel* **57**, 533–540.
- Roy R., Hill V. G., and Osborn E. F. (1952) Polymorphism of Ga_2O_3 and the system $\text{Ga}_2\text{O}_3\text{-H}_2\text{O}$. *J. Amer. Chem. Soc.* **74**, 719–722.
- Ruble T. (1996) Geochemical investigation of the mechanisms of hydrocarbon generation and accumulation in the Uinta basin, Utah. Ph.D. dissertation, University of Oklahoma.
- Sanderson R. T. (1976) *Chemical Bonds and Bond Energy*. Academic.
- Sandvik E. I., Young W. A., and Curry D. J. (1991) Expulsion from hydrocarbon sources: The role of organic absorption. *Org. Geochem.* **19**, 77–87.
- Schmidt V. and McDonald D. A. (1979) The role of secondary porosity in the course of sandstone diagenesis. *Soc. Econ. Paleontol. Mineral. Spec. Pub.* **26**, 175–207.
- Schoonen M. A. A. and Barnes H. L. (1988) An approximation of the second dissociation constant for H_2S . *Geochim. Cosmochim. Acta* **2**, 649–654.
- Seewald J. S. (1994) Evidence for metastable equilibrium between hydrocarbons under hydrothermal conditions. *Nature* **370**, 285–287.
- Siskin M., Brons G., Katritzky A. R., and Balasubramanian M. (1990) Aqueous organic chemistry. 1. Aquathermolysis: Comparison with thermolysis in the reactivity of aliphatic compounds. *Energy & Fuels* **4**, 475–482.
- Skripka V. G. and Boksha O. A. (1976) Solubility of water in individual n-alkanes and their mixtures at elevated temperatures and pressures. *Tr. Vses. Neftegazov. Nauchno-Issled. Inst.* **61**, 96–110.
- Solomon P. R., Serio M. A., Despande G. V., and Kroo E. (1990) Cross-linking reactions during coal conversion. *Energy & Fuels* **4**, 42–54.
- Song C., Saini A. K., and Schobert H. H. (1994) Effects of drying

- and oxidation of Wyodak subbituminous coal on its thermal and catalytic liquefaction. Spectroscopic characterization and product distribution. *Energy & Fuels* **8**, 301–312.
- Sourirajan S. and Kennedy G. C. (1962) The system H₂O-NaCl at elevated temperatures and pressures. *Amer. J. Sci.* **260**, 115–141.
- Spiro B. (1984) Effects of the mineral matrix on the distribution of geochemical markers in thermally affected sedimentary sequences. *Org. Geochem.* **6**, 543–559.
- Srivastava R. D. and Farber M. (1978) Thermodynamic properties of group 3 oxides. *Chem. Rev.* **78**, 627–638.
- Stalker L. (1994) Interaction of water with sedimentary organic matter in the laboratory: Implications for the generation of oxygenated species (including CO₂) in sedimentary basins. Ph.D. dissertation, Univ. Newcastle upon Tyne.
- Stalker L., Farrimond P., and Larter S. R. (1994) Water as an oxygen source for the production of oxygenated compounds (including CO₂ precursors) during kerogen maturation. *Org. Geochem.* **22**, 477–486.
- Stout N. D., Koskinas G. J., Raley J. H., Santor S. D., Opila R. L., and Rothman A. J. (1976) Pyrolysis of oil shale: Effects of thermal history on oil yield. *Quarter. Color. Sch. Mines* **71**, 153–172.
- Sutton C. and Calder J. A. (1974) Solubility of high-molecular-weight n-paraffins in distilled water and seawater. *Environ. Sci. Technol.* **8**, 654–657.
- Sunberg E. M., Unger P. E., and Larsen J. W. (1987) Relation between tar and extractables formation and cross-linking during coal pyrolysis. *Energy & Fuels* **1**, 305–308.
- Tannenbaum E. and Kaplan I. R. (1985) Low-molecular-weight hydrocarbons generated during hydrous and dry pyrolysis of kerogen. *Nature* **317**, 708–709.
- Tannenbaum E., Huizinga B. J., and Kaplan I. R. (1986) Role of minerals in thermal alteration of organic matter—II: A material balance. *Amer. Assoc. Petrol. Geol. Bull.* **70**, 1156–1165.
- Teerman S. C. and Hwang R. J. (1991) Evaluation of liquid hydrocarbon potential of coal by artificial maturation techniques. *Org. Geochem.* **17**, 749–764.
- Tissot B. (1969) Premieres donnees sur les mecanismes et la cinetique de la formation du petrole dans les sediments simulation d'un schema reactionnel sur ordinateur. *Rev. Inst. Franc. du Petrole* **24**, 470–501.
- Tissot B. P. and Welte D. H. (1984) *Petroleum Formation and Occurrence*. Springer-Verlag.
- Townsend S. H., Abraham M. A., Huppert G. L., Klein M. T., and Paspek S. C. (1988) Solvent effects during reactions in supercritical water. *Ind. Eng. Chem. Res.* **27**, 143–149.
- Tsonopoulos C. and Wilson G. M. (1983) High-temperature mutual solubilities of hydrocarbons and water. Part 1: Benzene cyclohexane and n-hexane: *AIChE J.* **29**, 990–999.
- Ungerer P. (1993) Modelling of petroleum generation and expulsion—an update to recent reviews. In *Basin Modelling: Advances and Applications* (ed. A. G. Dore), pp. 219–232. Elsevier.
- Ungerer P. and Pelet R. (1987) Extrapolation of the kinetics of oil and gas formation from laboratory experiments to sedimentary basins. *Nature* **327**, 52–54.
- Ungerer P., Behar E., and Discamps D. (1983) Tentative calculations of the overall volume expansion of organic matter during hydrocarbon genesis from geochemistry data: Implications for primary migration. In *Advances in Organic Geochemistry 1981*, pp. 129–135. Wiley.
- Vernon L. W. (1980) Free radical chemistry of coal liquefaction: Role of molecular hydrogen. *Fuel* **59**, 102–106.
- Wagman D. D., Kilpatrick J. E., Taylor W. J., Pitzer K. S., and Rossini F. D. (1945) Heats, free energies, and equilibrium constants of some reactions involving O₂, H₂O, C, CO, CO₂, and CH₄. *J. Res. Natl. Bureau Stand.* **34**, 143–161.
- Weitkamp A. W. and Gutberlet L. C. (1970) Application of a microretort to problems in shale pyrolysis. *Ind. Eng. Chem. Process Des. Develop.* **9**, 386–395.
- Wen C. S. and Kobylinski T. P. (1983) Low-temperature oil shale conversion. *Fuel* **62**, 1269–1273.
- Whitehouse B. G. (1984) The effects of temperature and salinity of the aqueous solubility of polynuclear aromatic hydrocarbons. *Mar. Chem.* **14**, 319–332.
- Whitney G. (1990) Role of water in the smectite-to-illite reaction. *Clays Clay Mineral.* **38**, 343–350.
- Williams L. A. and Crerar D. A. (1985) Silica diagenesis. II. General mechanisms. *J. Sediment. Petrol.* **55**, 312–321.
- Wyllie P. J. (1977) Effects of H₂O and CO₂ on magma generation in the crust and mantle. *J. Geol. Soc. London* **134**, 215–234.
- Yates J. T. and McKee D. W. (1981) Kinetic isotope effect in the heterogeneous reaction of graphite with H₂O (D₂O). *J. Chem. Phys.* **75**, 2711–2714.